Barnegat Bay—Year 2

Dr. Marina Potapova, Academy of Natural Sciences of Drexel University, Principal Investigator

Nina Desianti, David Velinsky, Jerry Mead, Academy of Natural Sciences of Drexel University, Co-Principal Investigators

Project Managers:
Mihaela Enache and Tom Belton,
Division of Science, Research and Environmental Health

Thomas Belton, Barnegat Bay Research Coordinator

Dr. Gary Buchanan, Director—Office of Science

Bob Martin, Commissioner, NJDEP

Chris Christie, Governor

June, 2015

Barnegat Bay Nutrient Inference Model

FINAL REPORT

DRAFT

Prepared for:
New Jersey Department of Environmental Protection
Mihaela Enache and Thomas Belton
428 E. State Street
Trenton, N.J.08625-0420
609-633-3866

Prepared by:
Academy of Natural Sciences of Drexel University
Marina Potapova
Nina Desianti
David Velinsky

1900 Benjamin Franklin Parkway
Philadelphia, PA 19103

April 6, 2015

TABLE OF CONTENTS

TABLE OF CONTENTS (cont)

LIST OF TABLES

LIST OF FIGURES

Executive Summary

There is an on-going discussion on whether eutrophication is causing algal blooms and increased macrophyte growth, which are presumably causing documented secondary detrimental side effects (i.e., anoxia, loss of submerged aquatic vegetation, increase in jelly fish, decreases in fish and crab population, etc) in the Barnegat Bay, New Jersey. The discussion revolves around the fact that Barnegat Bay has historically been poorly drained, and that what we may see as current eutrophication effects is only a part of natural conditions exacerbated by current nitrogen loading (i.e., with some of the negative effects coming from other stressors such as increased boat and jet ski traffic, bulkhead increases, loss of freshwater flows due to regionalization of upstream river sewerage treatment plants and loss through municipal ocean outfall, etc).

The New Jersey Department of Environmental Protection (NJDEP) is evaluating the appropriate indices to be used to measure the ecosystem health of New Jersey's shallow, lagoonal estuaries or coastal bays. These would include bays such as Great Bay, Great Egg Harbor Bay, Absecon Bay, Ludlam Bay and Barnegat Bay. The federal government (USEPA and NOAA) has already developed a suite of indicators (e.g., EPA 2012 and NOAA's National Estuarine Eutrophication Assessment update) and has applied them to NJ's coastal bays with mixed results, especially as state level management tools, due to both geographic scale issues and the inability of the USEPA and NOAA metrics to identify proximate sources and causes of impairments.

Further information is needed for NJDEP to develop water quality management tools; this study is designed to directly assist NJDEP in the development and/or enhancement of its nutrient criteria. There is growing consensus that the traditional macroinvertebrate indices used in EPA's EMAP and National Coastal Assessment may not be adequate to fully characterize the ecosystem health of shallow lagoonal estuaries such as those along the New Jersey coast. Together with macroinvertebrates, diatoms, which are microscopic siliceous algae, are commonly used as indicators of environmental conditions in aquatic ecosystems. Diatoms are widely used to monitor ecosystem health in freshwater ecosystems, but investigations have been started to develop diatom-based environmental indicators in coastal systems, too.

The goal of this project was to develop diatom indicators of ecosystem health in Barnegat Bay. This was accomplished by investigating how diatom assemblage composition varied along the gradients of sediments contaminants and nutrients, and how marsh diatoms changed since the time of European settlement. A subset of surface sediment samples collected from 50 sites in Barnegat and Great Bays in 2012 was used to measure contaminant concentrations and to relate diatom species distribution to contaminants. The contaminant concentrations were mostly below published sediment quality guidelines and exceeded them only in a few locations in the northern part of the Barnegat Bay. Various contaminants, such as metals, PAHs and PCBs were strongly correlated with each other and were generally higher in fine-grained sediments rich in organic matter. There was a statistically significant relationship between contaminant concentration and diatom assemblage composition, but the effect of individual contaminants on diatoms could not be distinguished because of the high correlation between contaminants.

The surface sediment sample set collected in 2012 from 100 sites in Barnegat Bay and Great Bays was re-analyzed using additional taxonomic data. Besides a strong gradient in the composition of diatom assemblages corresponding to the north-south gradient of land-use, salinity and other associated environmental variables, a statistically significant response of diatoms to sediment Carbon and Nitrogen was revealed. A model for inferring sediment Nitrogen content from the diatom assemblage data was constructed. Together with salinity model it is can be used for environmental assessments in lagoonal estuaries in New Jersey.

Five sediment cores were used to identify reference diatom assemblages and to reconstruct environmental conditions in Barnegat Bay marshes in the last 400 years. Four cores have been collected and analyzed previously, but new diatom and pollen data were added to the current analysis. The fifth core was collected in 2014 from a marsh in Great Bay, which is considered to be less impaired than Barnegat Bay. In most Barnegat Bay cores an increase of nitrogen content was evident in the course of the last 150 years, but such consistent trend was not found in Great Bay core. The pollen data show a peak of Ambrosia pollen associated with maximal land clearing around 1860s. The common trend for diatom assemblages in the cores was toward dominance of species indicative of relatively high sediment nitrogen content. The diatom species characteristic for relatively low sediment Nitrogen content and pre-1860 core intervals are considered as indicators of “reference” conditions in New Jersey marshes.

In summary, this study demonstrated that diatom assemblages are sensitive indicators of nutrients and contaminants in New Jersey lagoonal estuaries. Diatoms can be successfully used to reconstruct past environmental conditions and to monitor effect of environmental restoration programs. This can be done either by directly applying inference models to indicate nutrient enrichment or by developing a set of simple diatom indices based on species affinities towards low or high nutrient concentrations. Lessons learned from this project should be used to design further studies of responses of benthic communities to environmental stress in coastal areas.

A) Introduction

A1: *Background*

The New Jersey Department of Environmental Protection (NJDEP) is evaluating the appropriate indicators to be used to measure the ecosystem health of New Jersey's shallow, lagoon-type estuaries such as Barnegat Bay and Great Bay. The Barnegat Bay water quality is affected by persistent pollution impacts (eutrophication, algal blooms, low dissolved oxygen) (Kennish et al. 1984, 2007, Olsen & Mahony 2001). A suite of indicators have been developed by the USEPA and NOAA [(US EPA's National Coastal Assessment Report 2005 and NOAA's National Estuarine Eutrophication Assessment update (http://ian.umces.edu/neea/pdfs/dldo.pdf)] and have been applied to New Jersey's coastal bays with mixed results, due to geographic scale issues and the inability of the USEPA and NOAA metrics to identify proximate sources and causes of impairments (Velinsky et al. 2010c).

Bioindicators (e.g., phytoplankton, zooplankton, phytobenthos, zoobenthos) provide a powerful tool for water quality assessment in coastal regions under the influence of multiple stressors (e.g., urbanization, industrial and agricultural land use). Because of their sensitivity to such environmental stressors, they can be used successfully for monitoring the impact of human activities in coastal ecosystems. Extensive residential development increased the nutrient supply to Barnegat Bay (i.e., caused cultural eutrophication) which resulted in numerous adverse effects such as loss of biodiversity, episodic occurrences of algae blooms and brown tides, decline of hard clams and increasing number of invasive species (Kennish 2001). Despite the fact that nutrients from sewage have been diverted out of the Bay, the condition of Barnegat Bay has worsened over the last two decades. The impact of human-induced stressors and the biological, chemical, and physical processes responsible for habitat alteration in Barnegat Bay ecosystems are not fully understood. Thus, it is necessary to characterize the Barnegat Bay biota in terms of different kinds and degrees of impairment that are affecting its ecosystems.

Diatoms are photosynthetic protists found in nearly every freshwater and marine habitat and producing from 1/3 to 1/5 of the earth's atmospheric oxygen and organic matter (Armburst 2009). Assemblages of diatoms are proven robust indicators of stressors such as nutrients, acidification, and climate change. Diatoms are taxonomically distinct, abundant in most aquatic environments, and respond quickly to changing conditions. Because their silica shell, called

frustule, preserves in sediment deposits, diatoms are also widely used in assessing long-term environmental changes and the impacts of anthropogenic activities on aquatic systems and their watersheds. Diatom species are differentiated by their shape and characteristics of their siliceous skeleton. The main forms are centric (i.e., circular, radial symmetry), and pennate (i.e., having bilateral symmetry). They exhibit two main living modes in the environment: planktonic and benthic (i.e., living on or in the bottom substrate).

Diatoms inhabiting surface layers of sediments in estuaries and shallow coastal bays are important contributors to primary production in these ecosystems (Jonge & Van Beusekom 1992, 1995, Shaffer & Sullivan 1988, Varela & Penas 1985). They are also known to be sensitive to nutrients and other factors related to eutrophication (e.g., Admiraal 1977a, b, 1984, Underwood 2000). Diatoms from surface sediments of coastal areas have been successfully used to construct inference models and reconstruct eutrophication history (e.g., Cooper et al. 2010, Wekstrom 2006). Our previous study of sediment diatoms in surface sediments from Barnegat and Great Bays revealed major patterns of variation in diatom assemblage composition and diatom responses to nutrients (Potapova et al. 2013) and an investigation of four sediment cores from Barnegat Bay marshes demonstrated a consistent temporal change in diatom species composition during the last 400 years (Velinsky et al. 2010c). The next logical step is to combine the results of these studies to better understand how diatom assemblages are changing as a result of eutrophication and how they can be used to monitor environmental conditions.

Estuarine benthic diatoms are also known to be sensitive to heavy metals (Moreno-Garrido et al. 2003, Adams & Stauber 2004), but the whole-assemblage studies of the relations between diatoms and sediment contaminants have not yet been conducted. The surface sediment diatom samples collected in Barnegat Bay present a unique possibility to explore such relationships and possibility of using diatoms as indicators of various types of pollution.

A2: ***Objectives of Study***

The overall goal of this project is to incorporate a new biological component (diatoms) into ongoing water quality monitoring of Barnegat Bay coastal environments. This includes development and evaluation of diatom metrics indicating the condition of key ecological characteristics of the bay.

The objectives of the Year 1 project were to create a calibration set of diatom assemblages for developing inference models for the Barnegat Bay tidal wetland, embayment

and offshore ecosystems and to investigate the relationship between diatom indicators and anthropogenic influences in the watershed, such as urban and agricultural land use.

The first objective of the Year 2 project is to analyze data from five marsh sediment cores collected across the Barnegat Bay and in the Great Bay in order to reconstruct the history of environmental changes that occurred in the bays after European settlement. This work includes application of the diatom transfer functions developed in the Year 1 project and using other data on diatom ecology obtained in Year 1 as well as pollen data for paleoecological reconstructions.

The second objective is to investigate the relationships between diatom assemblages and contaminants in bay sediments using previously collected surface sediment samples.

A3: *Study Area*

The Barnegat Bay-Little Egg Harbor estuary (BB; Barnegat Bay) is located along the central New Jersey coastline in the Atlantic Coastal Plan province. Barnegat Bay is a barrier beach/back-barrier lagoon system from Point Pleasant south to Little Egg Inlet. The variety of highly productive shallow water and adjacent upland habitats found in this system include barrier beach and dune, submerged aquatic vegetation (SAV) beds, intertidal sand and mudflats, salt marsh islands, fringing tidal salt marshes, freshwater tidal marsh, and palustrine swamps.

The Barnegat Bay-Little Egg Harbor estuary is composed of three shallow bays (Barnegat Bay, Manahawkin Bay and Little Egg Harbor) and is approximately 70 km in length and varies from 2- to 6-km wide and up to 7-m deep. The watershed covers an area of approximately 1700 km^2 and has been extensively developed over the past 70 years. The tidal waters cover approximately 280 km^2 with a ratio of watershed area to water area of 6.1. The Bay is a back barrier island lagoon system with three connections to the ocean (Manasquan, Barnegat, and Beach Haven inlets. The current land use (2006) of the watershed is agriculture (~1%), wooded/forest (~28%), tidal and non-tidal wetlands (~18%), urban areas (~20%) and open water (30%) (Lathrop & Haag 2007). Importantly, watershed development (urban area) has increased over time. From 1986 to 2006 the amount of urban land cover increased from 15 to up to 21% of the land area, while forested land cover has decreased (NJ DEP, see www.state.nj.us/dep/bmw/ReportOcean.htm; Lathrop 2004). The population of the watershed has increased substantially from the 1940s (40,000) to over 570,000 year round resident

currently (US Census Reports). During the height of the summer season the population can rise to approximately 1,000,000.

The Great Bay is located south from the Little Egg Harbor and is connected to the ocean via the Little Egg Inlet. The Great Bay is the estuary of the Mullica River and is comprised of open water, intertidal marshes, mudflats and sandflats. In comparison to the Barnegat Bay-Little Egg Harbor estuary, the Great Bay watershed is considerably less developed. Average water depth in the Great Bay is 1.5m. Extensive areas of the bay bottom are covered by benthic algae and seagrasses. The Mullica River - Great Bay estuary is a large, relatively pristine, unaltered estuarine system. It is believed to be the cleanest estuary in the corridor from Boston to Washington, D.C., owing in large part to the fact that the majority of the watershed is protected by the Pinelands Management Area, several large federal and state wildlife management areas, and state forests. This productive estuary supports a high diversity of aquatic and terrestrial habitats and species, especially marine and estuarine fisheries populations, colonial nesting waterbird colonies on the salt marsh islands, migrating and wintering waterfowl, rare brackish and freshwater tidal wetland communities, plants, and invertebrates (Dowhan et al. 1997). Samples from the Great Bay were collected to represent reference conditions in contrast to samples from the Barnegat Bay-Little Egg Harbor that has considerably more developed watershed.

B) Field and Laboratory Methods

B1: *Sampling design*

For the analysis of sediment contaminants, 50 samples from the set of 100 surface sediment samples collected in 2012 were selected. These samples represented 50 open-water sampling sites distributed as equally along the Barnegat and Great Bays as possible (**Figure 1, Appendix 1**). Sites were selected to be as close as possible to the sites where benthic macroinvertebrates were sampled.

For the analysis of the historical changes in diatom assemblages the samples from five sediment cores were used. Four sediment cores were sampled in Barnegat Bay in 2009 and one new core from Great Bay, which represents a relatively undisturbed water body in comparison to Barnegat Bay, was collected in the course of this project. All cores were collected from marshes. Core locations are shown in **Table 1** and **Figure 2.**

B2: ***Field Sampling***

The field sampling in this project was limited to taking one sediment core from a marsh of the Great Bay. The core GB-2 was collected on May 20, 2014, at 39.51344 N and 74.41297 W in a mudflat (**Figure 3).** The core was collected using an acrylic tube and a tripod (**Figure 4).** The length of the core was 94 cm.

B3: ***Laboratory Methods***

B3.1: Core sectioning and dating

B3.1.1. *Core preparation*

The sediment core was brought to the laboratory in the tube and was sectioned into 1 cm (1 to 15 cm) or 2 cm (15 to 94 cm) sections (**Figure 5**). From each interval 2 cm^2 were subsampled for each diatom and pollen analysis, and the remaining was used for chemical and chronological analyses. Water content and sediment porosity was determined by change of weight of each sediment section after drying at 60°C. Dried sediment (5 to 45 g per section) was then counted on a Canberra high purity broad energy planar germanium detector with a 38 cm^2 active area for 24 hours. The activities of Pb-210 and Cs-137 in the samples were determined by the gamma peak areas at 46.5 and 661.6 keV, respectively. The instrument is calibrated against a standard of known activity (NIST Rocky Flats Soil Number 2; 4353A).

B3.1.2. *Cs-137 Activities and Calculated Sediment Accretion Rates*

The Cs-137 activity increased to a depth of 26 cm, below which Cs-137 rapidly declined to below detection (**Figure 6, Table 3**). The maximum Cs-137 activity (0.92 dpm/g) corresponds to the sediment deposited in 1964 when atmospheric fallout of Cs-137 was at its peak (Ritchie & McHenry 1990). The accretion rate of sediment deposited since 1964 can then be calculated from the depth at which the Cs-137 maximum depth is found. The Cs-137 dating method yields an accretion rate of 0.52 cm/yr (**Table 2**). There is no mechanism to systematically evaluate error in the Cs-137 based dating technique.

B3.1.3. *Pb-210 Activities and Calculated Sediment Accretion Rates*

Pb-210 activities were highest in the surface sediments (9.4 dpm/g maximum activity) and generally declined with depth, reaching a constant activity (1.27 dpm/g) from 40 to 90 cm (**Figure 7, Table 3**). The excess Pb-210 (Pb_{xs}) activity above the background activity, or 'unsupported' Pb-210, was calculated as the difference between the measured Pb-210 at each depth and the background Pb-210.

Two models describing Pb-210 activity with depth were used to determine accretion rates: the 'Constant Rate of Supply' (CRS) and 'Constant Initial Concentration' (CIC) models (Kolker et al. 2009). The CIC model assumes the Pb_{xs} activities are constant throughout the core, deposition rates are constant over time, and that the activity of sediment-associated Pb-210 deposited at the surface is constant over time. The shape of the Pb-210 profile with depth can then be described by:

$$A_x = A_o e^{\left(-\frac{\lambda}{s}\right)x}$$

where A_x is the Pb_{xs} activity at depth x, A_o is the initial Pb-210 activity, λ is the decay constant for Pb-210 (0.0301/yr), and s is the accretion rate (cm/yr). A single accretion rate can be derived for the entire core from the slope of the natural log of the Pb_{xs} against depth (**Figure 7):**

$$r = \frac{-\lambda}{s}$$

The slope of this regression (-0.070) yields an accretion rate (s) of 0.442 cm/yr (Table 1). Error in the CIC model derived accretion rates (σs) can be assessed through:

$$\sigma_s = s * \left(\frac{\sigma_{\lambda/s}}{r}\right)$$

where $\sigma_{\lambda/s}$ (0.005) is the error of the regression of the natural log of Pb_{xs} against depth (**Figure 8**). The CIC model therefore yields accretion rates of 0.442 ± 0.03 cm/yr (**Table 2**).

The CRS model does not assume constant accretion rates or initial concentrations, but only that the background Pb_{xs} is constant with depth. Depth-specific ages can be calculated

$$t_x = \frac{1}{\lambda} \ln \frac{Q_o}{Q_x}$$

where t is time (years), Q_x is the inventory of Pb_{xs} below depth x (cm), and Q_o is the total Pbxs inventory (Kolker et al. 2009), allowing for dating of specific sediment layers (**Figure 9).** Depth-specific sediment accretion can then be calculated by the differences in ages and depths of adjacent sediment sections (**Figure 10**):

$$s_x = \frac{x_i - x_{i-1}}{t_i - t_{i-1}}$$

The age of the sediment in the GB-2 core increased with depth to a maximum calculated age of 140.3 years at 52 cm, corresponding to the year 1874 (**Figure 9**). Sediment depth below 32 cm (corresponding to an age of more than 80 years) were not used in calculating depth-specific accretion rates or the whole-core average CRS accretion rate due to increased error of Pb-210 activities in sediments of this age. Depth-specific accretion rates ranged from a minimum of 0.23 to a maximum of 0.92 cm/yr (**Figure 10**). Error in the CRS model is evaluated against the ranges of depth-specific accretion rates. The weighted (for sediment section size) average accretion rate for the CRS data was 0.47 cm/yr (0.23-0.92; **Table 2**).

The accretion rate at GB-2 increased significantly over time (0.006 cm/yr per year; p = 0.001; **Figure 11**). Accretion rates in the 1940-1975 period averaged 0.26 (±0.04) cm/yr, and increased to 0.55 (±0.18) cm/yr in the 1975-2014 time period (**Figure 11**). This indicates that accretion at the GB-2 site increased from rates below the rate of relative sea-level rise (RSLR) in the region (0.41 cm/yr at Atlantic City, NJ) in the early part of the 20th century, to rates exceeding RSLR since the mid-1970s (**Figure 11**).

B3.2: Sediment Total Organic Carbon, Total Nitrogen and Total Phosphorus

Published laboratory clean-techniques were used throughout (US EPA 1997; APHA, AWWA and WEF 1995) using protocols as outlined in standard operating procedures (SOPS) at the Academy of Natural Sciences and University of Delaware (ANS 2012). All materials coming in contact with the samples were either glass or metal and were cleaned of any contaminants prior to use. Sample ID forms were used and each sample was given a unique laboratory number

for sample tracking. Below are brief descriptions of each chemical, biological, or physical method.

Total organic carbon and total nitrogen were measured using a CE Flash Elemental Analyzer following the guidelines in EPA 440.0, manufacturer instructions and ANSP-PC SOP. Samples were pre-treated with acid to remove inorganic carbon.

Total sediment phosphorus was determined using a dry oxidation method modified from Aspila et al. (1976) and Ruttenberg (1992). Solubilized inorganic phosphorus was measured with standard phosphate procedures using an Alpkem Rapid Flow Analyzer. Standard reference material and procedural blanks were analyzed periodically during this study. All concentrations were reported on a dry weight basis.

B3.3 Sediment isotopic analysis

Sediment samples were treated with fuming HCl to remove any possible inorganic carbon. This potential bias is small compared with the variations observed in many samples including this study.

Samples for isotopic analysis were analyzed using an Elemental Analyzer (NA2500) coupled to a Finnigan Delta Plus isotope ratio mass spectrometer (EA-IRMS). Samples were re-dried and were run in duplicate or triplicate where analytical variability was generally < 3% RSD. Multiple in-house standards were analyzed for each run to assess comparability over time. The within-run standard deviation of these multiple in-house standards was ±0.4‰ for $\delta^{15}N$ and ±0.2‰ for $\delta^{13}C$. Samples were reported in the standard (‰) notation:

$\delta X = (R_{sample}/R_{standard}) - 1) \times 1000$; where X is either ^{13}C or ^{15}N and R is either $^{13}C/^{12}C$ or $^{15}N/^{14}N$.

The $\delta^{15}N$ standard was air ($\delta^{15}N = 0‰$), and for $\delta^{13}C$ the standard is the Vienna PeeDee Belemite (VPDB) limestone that has been assigned a value of 0‰. Analytical accuracy was based on the standardization of scientific grade N_2 and CO_2 used for continuous flow-IRMS with International Atomic Energy Agency's (IAEA) N-1, N-3 and USGS 26 for nitrogen and IAEA's sucrose, National Institute of Standards and Technology's (NIST) NBS 19 and NBS 22 for carbon, respectively.

B3.4: Sediment contaminants

B3.4.1 *Organic Contaminants (PCBs, PAHs, selected OC pesticides)*

Subsamples were mixed with Na_2S0_4 to eliminate water and extracted with dichloromethane using a Soxhlet extractor for 18 h. In the remaining portion of the extracts prepared for contaminant analyses. Solid-liquid chromatograph using florisil (hexane as the eluent) was performed as an additional clean-up step to remove lipids and other compounds. PAHs were quantified using a capillary gas chromatograph coupled with a mass spectrometer in the electron impact mode after a clean-up procedure employing liquid-solid chromatography with alumina as the stationary phase (Ashley & Baker 1999). After PAH determination, samples were further cleaned using liquid-solid chromatography with florisil as the stationary phase. Internal standards were added to all the samples and calibration standards prior to instrumental analysis: 2,3,6-trichlorobiphenyl (CB30) and 2,2',3,4,4',5,6,6'-octachlorobiphenyl (CB204) for PCBs. One hundred and eleven PCB congeners, either singly or co-eluting, were analyzed using a Hewlett Packard 6890 gas chromatograph equipped with a ^{63}Ni electron capture detector and a 5% phenylmethyl silicon capillary column. The carrier and make-up gases were hydrogen and argon/methane, respectively. The temperature program began with 100^{o}C for 2 min, 100-170 ^{o}C at 4^{o}C min^{-1}, 170- 280^{o}C at 3^{o}C min^{-1}, and 5 min at 280 °C. The injector and detector temperatures were 225 and 285°C, respectively. Two-microlitre samples were injected with an auto sampler (HP 7673) in the splitless injection mode.

The identification and quantification of PCB congeners followed a previously published method (Swackhamer, 1987) in which the identities and concentrations of each congener in a mixed Aroclor standard (25: 18:18 mixture of Aroclors 1232, 1248 and 1262) were determined by calibration with individual PCB congener standards. Reported concentrations are for the sum of 110 congeners (some co-eluting expect for congener 1 and 3), 40 aromatic hydrocarbons (not including naphthalene) and 22 pesticides (i.e., DDXs, chlordanes, BHC and others).

B3.4.2 *Trace Metals*

Trace metals were digested and analyzed at the Geochemical and Environmental Research Group (GERG) which is part of Texas A&M University. In brief, before samples can be analyzed they must be converted from solid to liquid form using an acid digestion. Wet samples are homogenized in their container, and an aliquot is freeze dried and homogenized to a fine powder. Approximately 1.00 gram of powdered sediment is weighed into a beaker. Then HNO_3 and H_2O_2 (or other acids if necessary) are added and the mixture is heated at 95^{o}C. After

this acid digestion, the digestate is diluted to specific volume with reagent water, mixed and either filtered or allowed to settle overnight before analysis if required. The solutions are then analyzed for trace metals using appropriate instrumental method (ICP-OES or ICP-MS). This method is not a total digestion technique. It is a very strong acid digestion that will dissolve many elements that could become "environmentally available." Elements bound in silicate structures are not normally dissolved by this procedure, and are not usually mobile in the environment.

B3.5: Diatom identification and enumeration

About 1g of sediment from each sediment sample was used for diatom sample processing. The organic component was oxidized with 70% nitric acid while heated in a CEM microwave (165ºC) for 1.5 h. Diatoms were repeatedly allowed to settle for 24 hours and the supernatant was decanted until it reached a neutral pH. A measured amount of digested sample was dripped onto a microscope cover slip and dried. Cover slips were then mounted onto slides using a high refractive index mounting medium (Naphrax™). Diatoms were counted and identified using a Nikon Eclipse 80i microscope equipped with DIC optics. Five hundred valves were counted for each slide at 1000x magnification. More details on standard operating procedures for diatom analysis can be found in "Protocols for the analysis of algal samples collected as part of the USGS National Water Quality Assessment Program" (Charles et al. 2002; http://diatom.ansp.org/nawqa/protocols.asp). Diatom species identifications were made using the extensive diatom library at ANSP Diatom Herbarium. The references that were most commonly consulted were diatom floras of the marine coasts and brackish waters (Cooper 1995b, Snoejis 1993, Snoejis & Balashova 1998, Snoejis & Kasperovicene 1996, Snoejis & Potapova 1995, Snoejis & Vilbaste 1994, Witkovsky et al. 2000). Scanning electron microscopy (SEM) was used to identify the smallest diatoms and to clarify taxonomic placement of many unknown species. For SEM samples were air-dried on aluminum stubs, sputter-coated with platinum-palladium using a Cressington 208HR sputter coater and examined with a Zeiss Supra 50VP SEM operated at 10 kV at the Centralized Research facility, Drexel University.

Diatom data previously generated for several samples from four cores collected from Barnegat bay marshes in 2009 we re-analyzed. The initial identification of diatoms in these samples was based strictly on light microscope observations. The data generated in this project are backed by new taxonomic information from scanning electron microscopy observations. The

previously counted slides were revisited and in most cases recounted. The diatom count data generated in Year 1 stage of this project were also corrected based on extensive SEM studies of the samples.

B3.6: Pollen Analysis

Pollen samples were processed at the Texas A&M University palynological laboratory by Dr. Vaughn Bryant following the standard acetolysis technique of Faegri & Iversen 1989. A total of 2 cm2 of sediment was used for processing. Lycopodium was used as a marker for calculation of pollen species absolute abundances.

Identification and enumeration of pollen grains was done by Dr. Vania Stefanova, University of Minnesota). Pollen and spores were counted under a light microscope at 400X magnification. Identification to the lowest possible taxonomic level was made with keys of McAndrews et al. (1973), Punt et al. (1976-2003), Moore et al (1991), Reille (1992-1998), Beug (2004), and the pollen reference collection at the University of Minnesota.

The identification of the non-pollen palynomorphs (NPP: fungal spores and algal colonies, followed van Geel et al. (1989) and van Geel and Aptroot (2006). Charcoal particles >20µm were counted as an indicator of fire (Tinner & Hu 2003).

Pollen percentages are based on the pollen sum (100%) of AP (arboreal pollen, including trees and shrubs) and NAP (non-arboreal pollen). In each sample at least 300 terrestrial pollen grains were identified. Pollen of Cyperaceae, aquatic plants, and as well as spores of ferns, mosses, and fungi were excluded from the sum.

B3.7: Data Analysis

To find out major gradients in the diatom species dataset, a series of Detrended Correspondence Analyses (DCA) were performed. DCA is based only on species data, but correlations of environmental variables with DCA axes may be correlated and plotted as it was done here to visualize the correspondence between variation in species data and the environment.

Canonical Correspondence Analyses (CCA) were carried out to determine the strength of the relationships between diatom assemblage composition and specific environmental variables, either one at a time, or several selected by the forward selection procedure. Unlike DCA, which

is a strictly exploratory analysis, CCA allows statistical testing of effects of environmental parameters on biological assemblages.

All ordinations were carried out with the CANOCO 5.0 software (Ter Braak and Smilauer 2012). Species data were square-root transformed as it is usually done for proportional data. Environmental variables that had skewed distributions were log-transformed. These included all nutrient and chlorophyll A data. Land-use variables were square-root transformed because they were expressed as percentages. All analyses that included species data were repeated with all-species datasets (with and without down-weighing of rare species) and with a dataset that included only species that reached 1% relative abundance in at least 5 samples. The latter analyses were carried out to decrease noise in the species data.

Inference models were constructed for all variables and diatom datasets pairs where CCAs recovered response significant at p= 0.001. This significance level was chosen because it is the strictest criterion allowed by the software. These analyses used 2 species datasets: (1) all species and (2) only those species that reached 1% relative abundance in at least 5 samples and three sites datasets: all 100 sites, marsh sites, and open-water sites for a total of 6 pairs of datasets. Five kinds of modeling approaches were used: (1) Weighed Averaging with classical de-shrinking, (2) Weighed Averaging with inverse de-shrinking, (3) Weighed Averaging- Partial Least Squares, (4) Maximum Likelihood regression and calibration, and (5) Modern Analog Technique. Bootstrapping was used to validate the models. The measures of model performance are the bootstrapped coefficient of determination (R^2_{boot}) and the root-square mean error of prediction (RMSEP). Inference models were constructed using C2 software (Juggins 2003).

To reconstruct environmental conditions in Barnegat and Great Bays the inference models developed from the 2012 calibration dataset were used. These analyses were done in the C2 software (Juggins 2003). To delineate microfossil-based zones, the depth-constrained clustering analysis (CONISS) was implemented in the the Rioja package for R (Juggins 2014) and Tilia 1.7.16 program (Grimm 2011).

C) Results and Discussion

C1: *Sediment Contaminants*

Detailed data on sediment contaminants are given in **Appendix 1**, while the summary data is presented in **Table 4**. The concentrations of lead (Pb), total PAHs (40 compounds) and total PCBs (110 congeners) are presented in **Figure 12**. The distributions of these parameters are

indicative of the other contaminants within the Barnegat and Great Bays. In general, higher concentrations of many particle-associated contaminants are found with fine-grained sediments rich in organic matter (i.e., organic carbon). As the concentration of organic matter increases, the sorption capacity and affinity of PCBs and PAHs for sediment also increases, thereby promoting deposition of the contaminants on the bay bottom. Trace metals also have an affinity for fine grain sediments in many cases dependent on the mineral phase present (e.g., iron-manganese oxides, sulfides, carbonates, etc). While beyond the scope of this project, these factors need to be considered in understanding the source and concentrations patterns in the bays.

Lead concentrations ranged from 2.9 to 90 μg/g dw with an overall average of 21μg/g dw (**Table 4**). Concentrations were highest in the upper bay (peak concentration of 90 μg/g dw) and near the Toms River area (peak concentration of 63 μg/g dw). Lower concentrations were observed in the lower bay (< 25 μg/g dw). Similar concentrations were observed by the intensive study by Moser & Bopp (2001) and recently by Fischer et al. (in press). There was a significant relationship between iron (a tracer of grain size and non-anthropogenic metals) and lead with only a few outliers (**Figure 13**). This suggests that there are no specific direct sources of lead to the bays (i.e., point sources) and that watershed runoff and estuarine mixing are result in the overall distribution. Higher concentrations are found in the more developed areas of the Barnegat Bay; importantly the numerous marinas in the bay, especially in the northern areas could be a direct source to bay waters (Kennish 1994; Moser & Bopp, 2001; Vane et al. 2008).

PAH's can enter the bays environment from various pathways (direct and indirect) including sewage runoff, direct oil spills, and the combustion of fossil fuels. Urban and agricultural runoff and direct discharges can introduce PAHs (and other hydrocarbons) to bay (Kennish 1994; 2002). Polycyclic aromatic hydrocarbons (PAHs) were detected in all samples analyzed. PAHs comprised 40 individual compounds ranging from the low molecular weight compounds such as naphthalene and phenanthrene (2- and 3-rings) to high molecular weight compounds with 4- and 5- rings, including pyrene and dibenz[a,h]anthracene. While the pattern of individual PAH compounds can help with source identification, for this report, only the sum of the individual PAH compounds are presented.

Total PAHs (methyl-substituted and un-substituted forms) ranged from 0.02 to 7.2 μg/g dw (**Table 4; Appendix 1**) with a similar distribution as other chemical contaminants in the Barnegat and Great Bays (**Figures 1 and 13**). It should be noted that concentrations below approximately 5-8 ng/g dw are nearer the detection limit of the method. Concentrations were

highest in the northern, more developed areas, of the Barnegat Bay, again near Toms River and substantially lower in the lower portions of the bay. Overall, concentrations reported in this study appear higher than those reported in Moser & Bopp (2001), although further examination of the summary data needs to be undertaken. It is not clear if similar compounds were summed for total PAHs, however the study recently completed by the Fischer et al. (in press) showed similar concentrations and overall distribution.

Polychlorinated biphenyls (PCBs) were mainly produced by the Monsanto Corporation from 1930 to 1977 and it is estimated that 5.4×10^8 kg has been produced within the United States (Kennish 1992). They are or have been used as electrical insulators in many transformers, fire retardant, and additives to oils and paints. There are 209 congeners (or compounds) of PCBs based on the position and number of chorines on the biphenyl structure. The physical and chemical properties of this group of congeners vary greatly in the environment (ATSDR 2000). Persistence of PCBs in aquatic sediments is due to their slow rate of degradation and vaporization, low water solubility, and partitioning to particles and organic carbon. Bacteria degrade PCB, with the rate dependent on the position and degree of chlorination of the biphenyl ring and in many cases the absolute concentration present in the sediments (Kennish 1992 and others). Current sources to this area are thought to be from contaminated sites, runoff from old landfills and accidental spills (e.g., transformer fluids). In addition, PCBs can enter the bays from source areas such as urban/watershed runoff, potential contaminated site runoff, and direct atmospheric deposition.

Total PCBs ranged from 0.7 to 89 ng/g dw throughout the Barnegat and Great Bays (**Table 4, Appendix 1**). Highest concentrations were found at Metedeconk River near Brick with substantially lower concentrations down bay (<15 ng/g dw). Concentrations are similar to those recently reported by the Fischer et al. (in press) overall with a similar distribution. There was a significant relationship ($r2 = 0.842$, $p<0.001$) between the organic carbon content and total PCBs in the sediments throughout the Barnegat and Great Bays suggesting no specific point source in the bays and that particle transport is a major factor in the overall distribution of PCBs (and most likely other contaminants).

The contaminants measured in this study were compared to the published sediment quality guidelines (ERL and ERM; Long et al. 1995). The ERLs and ERMs are based on invertebrate toxicity (amphipods) not algae and are used to serve only as a guide to assess the levels within the bay to larger sediment guidelines. For trace metals, no location had

concentrations above the ERM. There were concentrations that exceeded the ERL for arsenic (48% of stations), cadmium (2% of stations), copper (6% of stations), lead (9% of stations), and zinc (13% of stations); with most stations in the upper bay. For total PCBs, only 4 out of 54 stations had concentrations above the ERL and none above the ERM, similarly only 3 our 54 stations (5% of stations) were above the total PAH-ERL (4.0 μg/g dw). Overall, concentrations are low compared to Long et al. (1995) published guidelines based on amphipod-derived data.

C2: *Great Bay Core analysis*

C2.1 Sediment Organic Carbon, Total Sediment Nitrogen and Total Sediment Phosphorus

Sediment organic carbon (OC) concentrations ranged from 2.8% to 6.4% on a dry weight basis (wt% dw) with an average of 4.3 ± 0.9% OC (± 1σ); **Table 6; Figure 14**). Similarly, total nitrogen (TN) ranged from 0.26 to 0.55% N with an overall average of 0.39 ± 0.08%; whereas total sediment phosphorus (TSP) ranged from 0.060 to 0.089% TSP with an overall average of 0.068±0.008%. These CNP concentrations (especially OC) are lower than those reported for BB-LEH (Velinsky & Sommerfield 2010) represent more mineral sediment deposited in this area. Data below will be presented as both depth and time changes.

Sediment total nitrogen and organic carbon concentrations were generally highest in the mid sections of the Great Bay core, between 20 and 70 cm (peak at ~ 1963), decreasing towards the surface with a minimum value at ~14 cm (~1985; **Figure 14).** Total phosphorus concentrations were similar at depth increasing to a sub-surface maximum and centered at 22cm (~1971). CNP concentrations increased from their minimum towards the surface with the largest increase for total phosphorus.

The carbon to nitrogen ratio (C/N; atomic units) can be used as a tracer of the source of organic matter to a location and potential diagenetic changes that could occur during burial (Marinucci 1982; Jasper & Gagosian 1990; Meyers 1994; Prahl et al. 1994). Diagenesis is any chemical, physical, or biological change undergone by sediment after its initial deposition (Berner 1980; Burdige 2006). In addition, sources such as terrestrial organic matter versus aquatic organic matter can be distinguished. For example, terrestrial material (e.g., trees) are rich in cellulose (i.e., higher C) compared to algae or marsh plants that have less structural material and are higher in proteins (i.e., higher N). Typical marine plants have C to N ratios of ~ 4-10 whereas terrestrial material can have C to N values > 15-20. Diagenesis of recent sediments tends to increase the C to N ratio due to preferential remineralization and release of nitrogen

compounds; however, re-incorporation of bacterially-derived N can increase the C to N ratio over time (Fogel et al. 1989; Benner et al. 1991).

In Great Bay, the C to N ratio (atomic) of the marsh sediment ranged from 9.5 at the surface to 15.3 at 32 cm (**Figure 14**). The general decrease from the maximum at 32cm (or 1955) towards the surface might indicate more aquatic marine sources of organic matter deposited on the marsh, however, degradation of organic matter cannot be ruled out at this point.

C2.2 Stable Isotopes of Carbon and Nitrogen

Organic carbon and nitrogen isotopic ratios are useful for distinguishing between marine and continental plant sources of sedimentary organic matter, processing and cycling of nutrients and, in some instances, the level of system-wide productivity (Fry 2006 and others). Most photosynthetic plants incorporate carbon into organic matter using the C3 Calvin pathway, which biochemically discriminates against ^{13}C to produce a $\delta^{13}C$ shift of about -20‰ to -30‰ from the isotope ratio of the inorganic carbon source. C4 plants (e.g., corn, *Spartina*) incorporate CO_2 using a different system (PEP) that discriminates against ^{13}C to produce a $\delta^{13}C$ shift of about -8‰ to -15‰ from the isotope ratio of the inorganic carbon source. Organic matter produced from atmospheric CO_2 ($\delta^{13}C$ of approximately –7‰) by land plants and typical tidal freshwater wetland plants, using the C3 pathway consequently has an average $\delta^{13}C$ (PDB) value of about -27‰ (O'Leary, 1988), although aquatic wetlands plants can have a large range (see Chmra & Aharon 1995; Malamud-Roam & Ingram 2001). In addition, the marsh plant *Juncus roemarianus* is a C3 plant and is reported to have $\delta^{13}C$ ranging from -23 to 26‰ (Haines 1976, Hughes & Sherr 1983; Chmra & Aharon 1995; Goñi & Thomas 2000). The source of inorganic carbon for marine algae (C3 plants) is dissolved bicarbonate, which has a $\delta^{13}C$ value of about 0‰. Therefore, marine organic matter consequently has $\delta^{13}C$ values between -20‰ and -22‰. The isotopic difference between organic carbon produced by C3 and C4 land plants and marine algae has been used to trace the delivery and distribution of organic matter to sediments in estuarine and coastal areas (Cifuentes et al. 1988, Fogel et al. 1992, Middleburg et al. 1997, Gebrehiwet et al. 2008 and others).

Carbon isotope ratios can be affected by photosynthetic dynamics and by post-depositional diagenesis (Dean et al. 1986; Fogel et al. 1992; Canuel et al. 1995, Zimmerman & Canuel 2002), thus isotope data must be interpreted cautiously. A big factor that can impact $\delta^{13}C$

values of plant material is the availability of CO_2 and rate of production during photosynthesis and the possibility of selective diagenesis of organic matter fractions that are isotopically heavy or light. Although the change in $\delta^{13}C$ appears to be small (<2‰) during recent diagenesis (Hayes et al. 1989, Meyers 1994), shifts due to the availability and rate of production, due to nutrient enrichment or limitation and other factors, can impact on the resultant $\delta^{13}C$ values of deposited organic matter (Ember et al. 1987, Fogel et al. 1992, Schelske & Hodell 1995; Church et al. 2006).

Differences exist between the natural abundances of stable nitrogen isotopes ($\delta^{15}N$, $^{15}N/^{14}N$) in dissolved and particulate matter from terrestrial, estuarine, marine, and anthropogenic sources (Kendall 1998). Terrestrial-occurring soil nitrogen can have a wide range of values, but in general range from -1 to +4‰) similar to atmospheric nitrogen (0‰). Nitrogen isotopic compositions from marine sources tend to be slightly enriched in the heaver isotope (^{15}N) and are very dependent on the source of dissolved nitrogen and its $\delta^{15}N$, and processing in the system (e.g., ammonification, nitrification, denitrification, etc) at the time of formation. A dominant process in many aquatic environments (and groundwater) is denitrification (Cline & Kaplan 1975). Denitrification is a microbially-facilitated process of dissimilatory nitrate reduction that ultimately produces molecular nitrogen (N_2) through a series of intermediate gaseous nitrogen oxide products. This microbial process uses dissolved nitrate during oxidation of organic matter and as nitrate is consumed there is an enrichment of residual nitrate in the system (i.e., $^{14}NO_3$ is preferentially consumed before $^{15}NO_3$). Algal/plant production and its $\delta^{15}N$ from nitrate would reflect the balance between processes and inputs. There are many points in which nitrogen can be fractionated and its isotopic composition altered. For example, wastewater from treatment facilities has been shown to increase the $\delta^{15}N$ of various fish species (Lake et al. 2001) due to the selective removal of the light isotope (^{14}N) nitrogen during treatment. Anthropogenic nitrogen was substantially enriched in watersheds with greater amount of urbanization and wastewater inputs and the nitrogen was shown to be incorporated into the aquatic food web (McCelland et al. 1997).

The isotopic compositions of sediment C and N exhibited interesting changes with depth (and time) within the Great Bay core (**Figure 15**). The carbon isotopic composition of the sediment ranged from -18.4 to -16.9‰ ($\delta^{13}C$ average of -17.6±0.4‰). Surface values (~-17.0 to -17.5‰) increased slightly with depth/time to approximately -18.4‰ within the root zone at approximately 12cm (early 1990s), below which values decreased generally with depth.

The $\delta^{15}N$ of the sediment increased substantially towards the surface from 2 to 2.8‰ at depth (<1830s) to a maximum of 4.6‰ at 30cm (ca. 1955). Above this maximum values decreased slightly to 3.7‰ at 15cm (ca.1985) and increased slightly to approximately 4.3‰ in the upper 3cm or about 2010.

In summary, the carbon isotopic signatures from the core are slightly enriched in ^{13}C compared to a *Spartina*- dominated system which might indicate some terrestrial inputs from the watershed and Mullica River. S*partina* is a C4 plant in which the organic carbon produced would have carbon signatures generally around -12 to -14‰ (Long et al. 1975). The values are generally similar to those found in Barnegat Bay area by Velinsky & Sommerfield (2010), but with a slightly different down core trend. Changes in the $\delta^{15}N$ of organic matter reflect potential changes in the source or cycling of nitrogen to Great Bay; similar to those observed in Barnegat Bay (Velinsky & Sommerfield 2010). In some studies this has been attributed to an increase in wastewater inputs, that have higher $\delta^{15}N$ signatures, increases in available nitrogen for plant growth, or to potentially increases in soil denitrification that would tend to increase residual $\delta^{15}N$ (Kendall 1988; Macko and Ostrom, 1994; McClelland et al; 1997; Lake, 2001; Wieben et al., 2013). The relationship between time and the changes in the carbon and nitrogen stable isotopes is presented in section C4.1 of this report.

C3: *Diatom ecology*

C3.1: Re-analysis of 2012 calibration dataset

C3.1.1: *Taxonomy*

The diatom counts generated during the Year 1 of this project have been re-analyzed to increase taxonomic resolution and thus to obtain better ecological characterization of taxa and assemblages. To that end many samples were studied using scanning electron microscopy (SEM), types of 44 species described from the US Atlantic coast in the past (Hohn & Hellerman 1996) were studied and most slides were re-visited and counts were corrected in the light of new information. These efforts led to the 50% increase in the number of diatom taxa in the calibration dataset, from 402 to 603.

C3.1.2 *Distribution patterns of diatom assemblages in space and along environmental gradients*

In order to check whether the count corrections had influenced the results of the Year 1 data analysis, we repeated the DCA and CCA ordinations using the 100-samples dataset with rare species down-weighting. **Figure 16** shows that as in the Year 1 analysis, the environmental variable that was most strongly related to diatom species composition was salinity and it was also highly correlated with Total Dissolved Phosphorus (TDP). The salinity gradient was also correlated with a gradient in land-use: from the most developed watershed in the north to the least developed in the south. In the comparison with Year 1 findings, the diatom response to such eutrophication-related parameter as water-column Chlorophyll A was more strongly correlated to the response to salinity, but the response to sediment carbon and nitrogen was independent from that to salinity and it was also stronger than in Year 1 analysis. This can be seen from the direction and the length of the arrow for sediment C and N (**Figure 16**).

C3.1.3 *Strength of diatom response to environmental factors*

The strength of the relationships between composition of diatom assemblages and environmental variables was measured by testing significance of the first canonical axes in a series of Canonical Correspondence Analyses (CCA). In each CCA, multivariate response variable was diatom assemblage composition, and a single explanatory variable was an environmental variable of interest. Significance of the response was measured by a Monte-Carlo permutation procedure, which was carried out simultaneously with CCA in CANOCO program. The summary of these analyses carried out with the species sets that included only species found at 1% relative abundance in at least 5 samples is given in **Table 7**. As in Year 1 analysis, in all three datasets of sites, which included 100-sites dataset, marsh-sites dataset, and an open water-sites dataset, the strongest responses of the diatom assemblages were to Salinity and Total Dissolved Phosphorus.

In order to determine whether an independent response to nutrients existed, a series of partial CCAs were conducted where environmental variables that showed significant effect in previous series of CCAs were used as constraints and salinity was used as a covariable. The results of these analyses are shown in **Table 8**. In the 100-sites dataset the response to sediment Nitrogen was the strongest among all eutrophication-related parameters. The responses in marsh and open-water datasets were weak because of the low number of samples.

C3.1.4: *Diatom inference models*

Inference models were constructed for all variables and diatom datasets pairs in 100 samples dataset where CCAs recovered response significant at p= 0.001. These analyses used 2 species datasets: (1) all species and (2) only those species that reached 1% relative abundance in at least 5 samples. Five kinds of modeling approaches were used: (1) Weighed Averaging with classical de-shrinking, (2) Weighed Averaging with inverse de-shrinking, (3) Weighed Averaging- Partial Least Squares, (4) Maximum Likelihood regression and calibration, and (5) Modern Analog Technique. Bootstrapping was used to validate the models. The ultimate measures of model performance are the bootstrapped coefficient of determination (R^2_{boot}) and the root-square mean error of prediction (RMSEP). Models constructed for the all- and reduced-species datasets did not differ significantly in their performance, and therefore, only models based on all-species datasets are reported here (**Table 9**).

The R^2_{boot} higher than 0.50 was observed only for models constructed for Salinity, Total Dissolved Phosphorus, Chlorophyll A, sediment Carbon and sediment Nitrogen (**Table 9, Figure 17**)**.** The Total Dissolved Phosphorus (TDP) model thus appears as the best one among all nutrient models in terms of its predictive power. The problem, however, is that considerable part of the variation in species data was explained by the interactions of Total Dissolved Phosphorus and Chlorophyll A with Salinity (**Table 10**). The joint effects of these variables with salinity are larger than the unique (conditional, marginal) effects of these eutrophication-related variables. This makes it difficult to ensure an independent response of diatoms to Chlorophyll A and TDP.

The sediment nitrogen model had a moderate predictive power (**Figure 17**), but the response to sediment N was stronger than to sediment C, and therefore this model was further considered. Since N and C are strongly correlated in sediments, it is difficult to ensure that the response is solely to Nitrogen and Carbon does not play any role, but both parameters could be related to eutrophication and therefore the variation of diatom assemblages along this environmental gradient is likely indicative of human impact. Together with Salinity model, the sediment N model was applied to the studied cores.

C3.2: Relationships between diatom assemblages and contaminants

The relationships between sediment contaminants and diatom assemblage composition was first explored by using the unconstrained ordination (Detrended Correspondence Analysis - DCA) method and then further quantified by the constrained ordination (CCA). As it has been

shown in Year 1 study that diatom assemblages in Barnegat Bay are strongly influenced by salinity and physical habitat, three variables, salinity, depth and sand content were also considered in the analyses. As grain size data were not available, sand content was estimated by visually inspecting the sample and this variable was coded on a 1-4 scale. Contaminant variables were nine metal concentrations and total amounts of PAHs and PCBs. In DCA, the diatom count data were used to reveal the major gradients in diatom assemblage composition and after the analysis the correlations of the DCA axes with 11 contaminant variables were calculated. The biplot of species scores and contaminant variables in the ordination space of the first and second DCA axes is shown in **Figure 18**. This plot shows that the major axis of diatom assemblage composition (DCA 1) to a large degree coincided with salinity and also with contaminant concentrations, which were strongly negatively correlated with salinity and also somewhat with sand content. For this reason, in the CCA analyses which were carried out to test for the significance of the relationships between diatom assemblages and contaminants, salinity and sand content were used as covariables. We used forward selection of variable to reduce the number of constraints in the CCA, so that only six variables that were significant at p=0.05 were used in the analysis. It does not mean, however, that other contaminants were not influencing diatom assemblage composition: their high correlations among each other made it impossible to separate their unique effects.

Although all selected variables had statistically significant influence on diatom assemblage composition, they together explained only 18% of variance in species data, which is expected in presence of other strong environmental gradients. **Figure 19** shows the CCA biplot of species and environmental (contaminant) variables resulting from this analysis. The second CCA axis reflects diatom assemblage variation along the gradient of contaminants concentration and species with low CCA 2 scores are indicative of cleaner sediments (**Table 11**), while those with high scores can be considered as relatively tolerant to contaminants (**Table 12**). It should be noted that species shown in Tables 5 and 6 were those that had relatively high (at least 2) weight in the CCA and had CCA 2 scores either the lowest or the highest quartile. These criteria are somewhat arbitrary and do not guarantee the best discriminatory power of metrics based on these lists. The best discriminating metrics can be identified using an independent set of samples.

C4: ***Paleoecological analysis of five marsh cores from Barnegat and Great Bays***

C4.1: Changes in nutrients concentrations with time based on sediment nutrients and isotope analysis

It is important to recognize that both nitrogen and phosphorus can undergo substantial biogeochemical processing and diagenetic changes during burial (see for example Berner, 1980; Howes et al., 1984; Hopkinson and Schubauer, 1984; Hines et al., 1989; Koretsky et al., 2008 and many others). In brief, inorganic forms of N and P are taken up by marsh plants, phytoplankton and benthic algae, and incorporated into marsh sediments. During burial, microbial activity (both oxic and anoxic) can release organic nitrogen and phosphorus into the porewaters of the sediments which can then move back into the overlying waters via advection and diffusion processes. A major sink or loss reaction for nitrogen is denitrification which converts oxidized nitrogen to nitrogen gas which is then removed from the system. These nutrients, along with externally introduced nutrients, are then transported to the Bay or taken up again during photosynthesis. This recycling of nutrients in a marsh is a major process that impacts overall marsh/estuarine productivity and transport to coastal areas. In this regard, depending on the environment and specific characteristics, such as the magnitude of nutrient loadings, sedimentation rates, oxic/anoxic conditions, it may or may not be possible to measure changes in nitrogen or phosphorus accumulation rates that reflect inputs from external sources as it is the case with chemicals that do not undergo significant biogeochemical reactions (e.g., PCBs, Pb, Zn, etc).

In Great Bay, total nitrogen and organic carbon varied over time (**Figure 14**). In general, TN concentrations varied slightly from 1830s to the 1960s and reached a minimum around 1975. At this time, TN increased to the present. During this time period, the isotopic composition of TN increased with time from approximately 2 to 4‰ (**Figure 15**). The OC profile was similar to that of TN with OC concentrations reaching a minimum around the mid-1970s, increasing slightly toward the present. With this decrease in OC concentrations, the δ13C decreased from -18.5‰ to approximately -17‰ near the surface. TP concentrations exhibited the biggest increase towards the surface with values approaching 0.1%.

Compared to Barnegat bay cores, the Great Bay core, in general had considerably lower TN and OC content (**Figure 20**). The stable isotopes of sediment nitrogen may give some indication as to changes in the source of nitrogen and biogeochemical cycling within the Bays. Ulseth & Hershey (2005), Leavitt et al. (2006) and Velinsky (unpublished data) show that higher $\delta^{15}N$ of the nitrogen is associated with higher inputs from urban sources, possibly wastewater

processes. Bratton et al. (2003) showed similar trends in cores from the Chesapeake Bay. Similarly, Elliot and Brush (2006) showed a correlation between the $\delta^{15}N$ of tidal wetland core sediments and estimates of nitrogen wastewater loadings over time. Lastly, in Woodbury Creek and Oldmans Creek marshes in New Jersey, an increase in $\delta^{15}N$ observed in sediment cores was attributed to both increased nitrogen loading and changes in the way nitrogen is processed in wastewater treatment plants (Church et al. 2006). However, in the Murderkill River marshes within Delaware Bay, there was a pronounced increase in the $\delta^{15}N$ of the sediment nitrogen in dated sediment cores (Velinsky et al. 2010abc). The increase in the $\delta^{15}N$, from < 2.5 ‰, near the bottom, to between 4 to 5 ‰ nearer surface, started in the 1950s and may be an indication of urban/suburban sources of nitrogen from the watershed. However, variations of $\delta^{15}N$ are somewhat difficult to interpret given the number of biogeochemical processes influencing nitrogen and variations of sources over time. In the Barnegat Bay (Velinsky & Sommerfield, 2010), starting in the early 1900s, there was a general increase in the $\delta^{15}N$ of sediment N. This was evident in the three upbay cores (BB-1, BB-2 and BB-3) with highest $\delta^{15}N$ of 2.7 to 3.9‰. At the downstream site, BB-4, even as the TN increased over time, the $\delta^{15}N$ decreased throughout the core (from ~4‰ to ~2‰ at present).

Concentrations of total sediment phosphorus (TSP) changed slightly over time, especially in the upper 30 cm (**Figure 14**). There was a sub-surface peak in sediment TP at approximately 1975 which generally correlates with the peak in phosphates in detergent use (Litke, 1999), after which there was a general decline in phosphorus inputs to aquatic environments. Interestingly, in the Great Bay core, sediment TP increased sharply towards the surface (**Figure 14**). It is unclear as to the source of this phosphorus to the Great Bay.

Schelske and Hodell (1991; 1995) and Perga and Gerdeaux (2004) have shown a relationship between the concentration of P in the sediments or water column and the isotopic composition of carbon ($\delta^{13}C$-OC) in the sediments or in fish scales over time, respectively. The fish scales were an integrator of the base of the food web (i.e., phytoplankton) and reflect nutrient inputs. Similarly, Church et al. (2006) showed a relationship between sedimentary P and $\delta^{13}C$-OC in a marsh core from Woodbury Creek, New Jersey. It is thought that as P levels increase, primary productivity increases to a point at which there is reduced isotopic fractionation during enzymatic uptake of dissolved CO_2. This reduced fractionation would result in higher isotopic compositions of organic matter (i.e., more ^{13}C-enriched) and would suggest that P was helping to control aquatic productivity. Therefore, if phosphorus is limiting

production, the $\delta^{13}C$ of the organic carbon in a core may reflect a system-wide change in productivity. However, while this relationship was shown in a tidal freshwater marsh (Woodbury Creek), it is has not been clearly evident in other tidal marshes, suggesting-site specific conditions may be most important (Velinsky et al. 2010abc). Other factors, such as the relationship between mineral and organic matter deposition within a marsh, organic matter decomposition and inputs of allochthonous material can be significant (Middleburg et al. 1997; Gebrehiwet et al. 2008).

In Barnegat Bay, there was no consistent trend in the $\delta^{13}C$ of organic carbon with time. However, in the Great Bay core there was a significant relationship between $\delta^{13}C$ of organic carbon and sediment TP (**Figure 15**); especially in the upper sections. This indicates that productivity within Great Bay over time can be assessed using a $\delta^{13}C$-TSP relationship as shown in Great Lake sediments (Schelske & Hodell (1991; 1995) and in Woodbury Creek (Church et al. 2006). It may be that P is controlling overall system productivity (see debate over nitrogen versus phosphorus in marine waters) or site-specific factors (e.g., low sedimentation rates; loading rates of N and P; see Conley et al. 2009) may be a factor.

C.4.2*:* Environmental changes inferred from diatom and pollen data

A pollen flora of 40 trees and shrubs and 27 herb taxa were determined in the studied cores, as well as fern spores (5 taxa), aquatics (6), algae (2), mosses (1), and some fungi (4). As stratigraphic diagrams (**Figures 21** and **22**) show, the pollen of ambrosia, which is considered as a marked of forest clearing considerably increased in all studied cores around 1860s. Time zones based on constrained clustering reflected this fundamental change in land-use. As it is known that maximum deforestation occurred in New Jersey around 1860s, our pollen data confirm Pb-210 dating of the cores.

In order to evaluate the degree of applicability of the inference models developed from the 2012 calibrations dataset (see section C3.1.4), we carried out an unconstrained ordination (DCA) using all samples from the calibration and core datasets. **Figure 23** shows that there is no overlap between envelopes drawn around samples from the calibration dataset and from Barnegat Bay marsh core samples and only some overlap with Great Bay core. The first ordination axis clearly separated samples from vegetated marshes (core samples) from those from mudflats, sandflats and subtidal zone (calibration dataset), while variation along the second

axis was obviously related to salinity, with samples from higher-salinity areas positioned in the upper part of the diagram and those from lower-salinity areas in the bottom part. Such separation between core samples and calibration samples is an indication that inference models may not be especially effective when applied to the cores. Still, there were many species common for both calibration and core datasets, therefore, the inference models were applied to core samples to infer salinity and sediment nitrogen content.

Figure 24 demonstrates that the trend in nitrogen content along the core BB-1 was well reflected by the trend in nitrogen inferred from the diatom assemblage data. This proves the utility of the diatom-based nitrogen inference model even in the situation when many species were different between calibration and core datasets. Diatom assemblages in New Jersey coastal ecosystem are so diverse, that there apparently there are enough species common for both datasets to infer environmental conditions in a habitat considerably different from that of the calibration dataset. Constrained cluster analysis revealed 2 major pollen zones and 3 diatom zones. The upper pollen zone was characterized by a marked increase in Ambrosia pollen and was positioned approximately at 1860 (**Figures 21** and **24**). This boundary coincided with a boundary between diatom zones 1 and 2. The largest shift in the diatom assemblage, however, occurred at about 1940, when the abundance of species indicative of the nitrogen enrichment considerably increased. The actual nitrogen content of sediments also increases after this boundary, confirming that northern part of the Barnegat Bay eutrophied especially fast in the second part of the 20^{th} century.

The trends were generally the same in core BB-2 (**Figure 25**). As in core BB-1, there were two pollen and three diatom zones, with the pollen zones boundary corresponding to the boundary between diatom zones 1 and 2 and the upper pollen zone characterized by the increase in Ambrosia (**Figure 21**). The difference with core BB-1 was in the dating of this boundary at about 1900 instead of 1860. The largest shift in the diatom assemblage was placed at about 1950 and similarly to the core BB-1 it was associated with an increase of nitrogen-tolerant species.

In the core BB-4, the increase of Ambrosia happens in the interval between 1820 and 1860 and again corresponds to the major shift in the pollen composition (**Figures 22** and **26**). The diatom assemblage appears to change with time more or less constantly towards dominance of nitrogen-tolerant species, while the major shifts in the species composition happened around 1880 and 1980.

The core GB-2 does not go as far back in time as cores BB-1, BB-2 and BB-4, so the increase in Ambrosia is not especially clear, but it can be seen from **Figure 22** that Ambrosia does increase in proportion between 1830 and 1860. Although nitrogen content did not present a clear temporal trend in this core, it is interesting, that it was quite well tracked by the diatom-inferred nitrogen values (**Figure 27**).

To summarize temporal trends in marsh diatom assemblages, a DCA was carried out that only included samples (101 in total) from the five cores (**Figures 28** and **29**). Positions of core enveloped in **Figure 28** demonstrate the importance of salinity in structuring marsh diatom assemblages: the cores are ordered along the first DCA axis, which is entirely aligned with an arrow representing salinity inferred from diatoms. The most "freshwater" is northernmost core BB-1, while the most "saline" is the core GB-2, with the whole sequence corresponding to the north-south salinity gradient. Only the core BB-3 taken from the mouth of Oyster Creek is slightly of order. The temporal variation within each core is, however, quite strongly related to the differences in abundance of Nitrogen- sensitive and Nitrogen-tolerant species. This can be seen from the closely positioned arrows for time and inferred nitrogen and the overall shape of the envelopes elongated in the same direction (**Figure 28**). The absence of considerable variation in sediment nitrogen and, therefore, in diatom species composition, in Great Bay core is reflected in the compact shape of its envelope.

Figure 29 represents the results of the same DCA in terms of the species scores. By using a LOESS modeling technique, we drew time isolines delineating assemblages characteristic for different time periods. The species that are separated by the 1860 isoline can be considered as indicators of relatively undisturbed conditions, since the direction of the temporal change coincides not only with time, but also with nitrogen content, presumably the result of eutrophication. The species that had the weight of at least 5 and had their nitrogen optima in the lower quartile were placed in the category "N-sensitive reference" species. The list of the "reference" diatoms included species representing different habitats and a range of salinity conditions: from diatoms characteristics for low-salinity marsh soils, such as *Cosmioneis pusilla, Diploneis smithii* and *Nitzschia brevissima*, to marine planktonic diatoms *Thalassionema nitzschioides, Thalassiosira striata* and *T. oestrupii* that settle on marshes soils when they are inundated by tides. These species are illustrated in **Figure 30**. The species with weight of 5 and greater and nitrogen optima in the upper quartile were considered "N-tolerant": these are illustrated in **Figure 31**. These species included small brackish-water planktonic diatoms such as

Cyclotella choctawacheeana and *C. marina* var. *gracilis*, which have been reported to increase in abundance with eutrophication (Cooper 1995a, b). Species that increased in abundance in lower-salinity cores include *Navicula gregaria* and *Planothidium frequentissimum*, which are known indicators of nutrient enrichment in inland waters (e.g., Potapova & Charles 2007). Among diatoms characteristic for more saline marshes, various species form the genera *Navicula*, *Nitzschia* and *Halamphora* were among the best indicators of eutrophication. For instance, *Navicula salinarum* that appears in our list of nitrogen-tolerant species has been also reported to respond to nutrient enrichment in experiments conducted by Sullivan (1975) in Delaware marshes. Various metrics suitable for monitoring eutrophication of the New Jersey coastal marshes can be constructed based on these two lists.

D) Summary and Conclusions

The main objective of this project was to determine how the surface sediment diatom assemblages may be used as indicators of ecosystem health in Barnegat Bay. We analyzed contaminants in 50 sediment samples and determined that diatoms assemblage composition is influenced by contaminants. We constructed inference models for inferring salinity and sediment nitrogen content from diatom data and applied them to marsh sediment cores. The diatom assemblages in the Barnegat Bay marshes shifted over time, and especially during the last 150 years, towards increased abundance of N-tolerant species. Our analysis revealed composition of diatom assemblages before these dramatic changes took place and the sets of diatom taxa were established that we recommend using as indicators of the "reference" or eutrophic conditions in New Jersey marshes.

<u>Major findings of this study include:</u>

- Total PAHs ranged from 0.02 to 7.2 μg/g of dry weight with the highest concentrations in the northern, more developed areas, of the Barnegat Bay, near Toms River, and substantially lower in the lower portions of the Barnegat and in the Great Bay.
- Total PCBs ranged from 0.7 to 89 ng/g of dry weight throughout the Barnegat and Great Bays. The highest concentrations were found at Metedeconk River near Brick with substantially lower concentrations down bay (<15 of dry weight).
- Metal concentrations were correlated with other contaminants and were also the highest in the northern part of the Barnegat Bay. Overall, contaminant concentrations were low compared to published guidelines.
- Benthic diatom assemblages showed a statistically significant variation along sediment contaminants gradient. List of diatom taxa indicative of relatively low and high contaminant concentrations were developed.
- Additional work on the taxonomy of coastal diatoms from New Jersey led to the re-analysis of the 2012 calibration dataset and allowed for the development of new inference models for salinity and sediment nitrogen content.

- In addition to four sediment cores collected in 2009 from Barnegat Nay marshes, a new core was taken in 2014 from a Great Bay marsh. This core was dated and analyzed for sediment CNP content, C and N isotopes, pollen and diatoms. Unlike Barnegat Bay cores, which were characterized by a marked increased of sediment nitrogen content in 20th century intervals, the Great Bay core did not show such an increase. This corresponds to the initial assessment of Greta Bay watershed as comparatively less impaired than Barnegat Bay. There was, though, a considerable increase of phosphorus in the uppermost intervals of the Great Bay core, which is presently difficult to interpret.
- Pollen was analyzed in four cores and in most of them there was a noticeable increase of Ambrosia pollen in the core depth intervals corresponding to 1860s. This increase is a marker of maximal deforestation that is known to occur in New Jersey approximately around 1860s.
- The analysis of diatom data showed that diatom assemblages were changing in all cores towards the prevalence of nitrogen-tolerant species in upper intervals, with major shifts in the mid-19th century and again around 1940s and often in 1980s. Nitrogen trend inferred from diatoms well tracked the actual nitrogen sediment values and we concluded that our ecological characterization of diatom species can be used for reconstructing past and monitoring current environmental conditions in New Jersey lagoonal estuaries. Lists of diatom species indicative of the "reference" and impaired conditions have been developed.

<u>Recommendations for Future Steps</u>

- To further develop diatom indicators of nutrient enrichment in the Barnegat Bay, we will repeat the statistical analyses of the calibration dataset after excluding sites that may be considerably influenced by the ocean water, such as Great Bay sites and also sites that are unusual in other environmental characteristics or in diatom species composition (outliers). We will also repeat all the analyzes after excluding the rare and planktonic species form the dataset using different sets of criteria from those used in Year 1 analysis.
- In addition to developing the transfer functions, we will determine diatom species

indicative of low and high concentration of total nitrogen and total phosphorus, separate for various habitats, such as marches and subtidal portions of the Bay.

- An additional work will be carried out to relate diatom species composition in cores to historical water quality data obtained from NJ DEP. This work will include data mining to extract usable water quality data and also a statistical analysis of the relationships between sediment diatoms and water-column nutrients.

- The grain-size data will be added to the set of environmental data and all exploratory analyses will be repeated to ensure that diatom response to contaminants and nutrients are not confounded by the grain size factor.

- C-14 data will be obtained during the Year 3 and will be added to the analysis of the cores.

- We will continue taxonomy work to publish descriptions of new species discovered in this project. This work will be useful for those wishing to use diatoms as environmental indicators along mid-Atlantic coasts.

-

E) Acknowledgments

We would like to thank several colleagues who carried out field sampling and laboratory analyses. Roger Thomas and his support team collected sediment the Great Bay core. William Frezel constructed the tripod for core collection and the extruder for sectioning the core. Paul Kiry, Paula Zelanko and Linda Zaoudeh carried out sediment chemistry analyses.

F) References

Academy of Natural Sciences. 2009. Quality Management and Quality Assurance Project Plan. Barnegat Bay Nutrient and Ecological Histories Core Collection and Analyses. Prepared for Mr. Thomas Belton, New Jersey Department of Environmental Protection (June 2009).

Academy of Natural Science. 2012. Quality Management and Quality Assurance Project Plan. Barnegat Bay Nutrient and Ecological Histories Core Collection and Analyses. Prepared for Mr. Thomas Belton, New Jersey Department of Environmental Protection (June 2012).

Adams, M.S. & Stauber, J.L. 2004. Development of a whole-sediment toxicity test using a benthic marine microalga. Environmental Toxicology and Chemistry 23: 1957–1968.

Admiraal, W. 1977a. Influence of various concentrations of orthophosphate on the division rate of an estuarine benthic diatom, Navicula arenaria. *Marine Biology* 42: 1-8.

Admiraal, W. 1977b. Tolerance of estuarine benthic diatoms to high concentrations of ammonia, nitrite ion, nitrate ion, and orthophosphate. *Marine Biology* 43: 307-315.

Admiraal, W. 1984. The ecology of estuarine sediment-inhabiting diatoms. *Progress in Phycological Research* 3: 269-322.

American Public Health Association, American Water Works Association and Water Environment Federation (APHA, AWWA and WEF). 1995. *Standard Methods for the Examination of Water and Wastewater*, 19th Edition. Washington, DC.

Appleby, P. G. & F. Oldfield. 1992. Application of lead-210 to sedimentation studies, in M. Ivanovich, and R.S. Harmon, eds., *Uranium-series disequilibrium; applications to Earth, marine, and environmental sciences*: Oxford, Clarendon Press, p. 731-778.

Armbrust, E.V. 2009. The life of diatoms in the world's oceans. *Nature* 459: 185-192.

Aspila, K.I, H. Aspila, A. Agemian and S.Y. Chau. 1976. A semi-automated method for the determination of inorganic and total phosphate in sediments. *Analyst* 101: 187-197.

Beug H-J. 2004. Leitfaden der Pollenbestimmung für Mitteleuropa and angrenzende Gebiete. Pfeil, Munich.

Bricker, S.B., Ferreira, J.G., and Simas, T. 2003. An integrated methodology for assessment of estuarine trophic status. *Ecological modeling* 169: 39-60.

Burdige, D.J. 2006. Geochemistry of Marine Sediments. Princeton University Press. 630 pp.

Charles, D.F., Knowles, C. and R.S Davis. 2002. *Protocols for the Analysis of Algal Samples Collected as Part of the U.S. Geological Survey National Water-Quality Assessment Program*. Patrick Center for Environmental Research-Phycology Section, The Academy of Natural Sciences of Philadelphia. Report No. 02-06. 124 pp.

Chumura, G.L. & P. Aharon. 1995. Stable carbon isotope signatures of sedimentary carbon in coastal wetlands as indicators of salinity regime. *J. Coast. Res*. 11: 124-135.

Church, T.M., C. Sommerfield, D.J. Velinsky, D. Point, C. Benoit, D. Amouroux, D. Plaa & O. Donard. 2006. Marsh sediments as records of sedimentation, eutrophication and metal pollution in the urban Delaware Estuary. *Marine Chemistry* 102(1-2): 72-95.

Cole, M., I. Valiela, K.D. Kroeger, G.L. Tomasky, J. Cebrian, C.Wigand, R.A. McKinney, Sara P. Grady, and Maria Helena Carvalho da Silva. 2004. Assessment of a d15N isotopic method to indicate anthropogenic eutrophication in aquatic ecosystems. *J. Environ. Qual*. 33:124–132.

Cooper, S.R. 1995a. Chesapeake Bay watershed historical land use: impact on water quality and diatom communities. *Ecological Applications* 5: 703-723.

Cooper, S. R. 1995b. Diatoms in the sediment cores from the mesohaline Chesapeake Bay, USA. *Diatom Research* 10: 39–73

Cooper, S.R. and G.S. Brush. 1993. A 2,500-year history of anoxia and eutrophication in Chesapeake Bay. *Estuaries* 16: 617-626.

Cooper, S.R., Gaiser, E., and Wachnicka, A. 2010. Estuarine paleoenvironmental reconstructions using diatoms. Pages 324-345 In: Smol, J.P. and Stoermer, E.F. (eds). *The diatoms: appicatios for the environmental and Earth sciences.* Cambridge, Cambridge University Press.

Dowhan, J., Halavik. T., Milliken, A., MAcLachlan, A., Caplis, M., Lima, K., and Zimba, A. 1997. Significant habitats and habitat complexes of the New York Bight watershed. U.S. Fish and Wildlife Service. Southern New England-New York Bight Coastal Ecosystems Program, Charleston, Rhode Island. Available online: http://library.fws.gov/pubs5/web_link/text/toc.htm.

Elliott, E.M. & G.S. Brush. 2006. Sedimented organic nitrogen isotopes in freshwater wetlands record long-term changes in watershed nitrogen source and land use. *Environ. Sci. Technol*. 40: 2910–2916.

Faegri, K. & Iversen, J. 1989. Textbook of Pollen Analysis, 4th ed. Wiley, Chichester.

Fisher, J.M. et al. In Press. Estuarine Bed-Sediment Quality Data Collected after Hurricane Sandy in New Jersey and New York, 2013— Study Design, Collection and Analyses Methods, Quality Assurance, and Data. USGS Report.

Fry, J., Xian, G., Jin, S., Dewitz, J., Homer, C., Yang, L., Barnes, C., Herold, N., and Wickham, J., 2011. Completion of the 2006 National Land Cover Database for the Conterminous United States, *PE&RS* 77(9): 858-864.

Ember, L.M., D.F. Williams & J.T. Morris. 1987. Processes that influence carbon isotope variations in salt marsh sediments. *Marine Ecology Progress Series* 36: 33-42.

EPA. 2012. National Coastal Condition Report IV. EPA-842-R-10-003. United States Environmental Protection Agency Office of Research and Development/Office of Water

Washington, DC. Available at http://water.epa.gov/type/oceb/assessmonitor/nccr/upload/0_NCCR_4_Report_508_bookmarks.pdf

Gehrels, W.R., Roe, H.M., and Charman,, D.J. 2001. Foraminifera, testate amoebae and diatoms as sea-level indicators I UK salt-marshes: a quantitative multiproxy approach. *Journal of Quaternary Science* 16: 201-20.

Grimm, E. C. 1991-2011: Tilia 1.5.11. Illinois State Museum, Research and Collections Center.

Hunchak-Kariouk, K. and R.S. Nicholson. 2001. Watershed contributions of nutrients and other nonpoint source contaminants to the Barnegat Bay–Little Egg Harbor Estuary. *Journal of Coastal Research Special Issue* 32: 28–81.

Janousek, C.N. 2009. Taxonomic composition and diversity of microphytobenthos in Southern California marine wetland habitats. *Wetlands*. 29: 163-175.

Jordan, T.E., J. C. Cornwell, W.R. Boynton, and J.T. Anderson. 2008. Changes in phosphorus biogeochemistry along an estuarine salinity gradient: The iron conveyer belt. *Limnology and Oceanography* 53: 172-84.

Jonge, V.N. and Van Beusekom, J.E.E. 1992. Contribution of resuspended microphytobenthos to total phytoplankton in the Ems estuary and its possible role for grazers. *Netherlands Journal of Sea Research* 30: 91-105.

Jonge, V.N. and Van Beusekom, J.E.E. 1995. Wind- and tide-induced resuspension of sediment and microphytobenthis from tidal flats in the Ems estuary. *Limnology and Oceanography* 40: 766-778.

Juggins, S. 2003. *C2 User guide. Software for Ecological and Palaeoecological Data Analysis and Visualization*. University of Newcastle, Newcastle upon Tyne.

Juggins, S. 2014. Package “rioja”. Available at http://cran.r-project.org/web/packages/rioja/rioja.pdf.

Kemp, A.C., Horton, B.P., Corbett, D.R., Culver, S.J., Edwards, R.J., and van de Plassche, O. 2009. The relative utility of foraminifera and diatoms for reconstructing late Holocene sea-level change in North Carolina, USA. *Quaternary Research* 71: 9–21.

Kennish, M.J. 1984. Summary and conclusions. In: Kennish, M.J. and R.A. Lutz (eds). *Lecture Notes on Coastal and estuarine studies. Ecology of Barnegat Bay, New Jersey*. New York, Springer Verlag, pp 339-353.

Kennish, M.J. 2001. Characterization of the Barnegat Bay-Little Egg Harbor estuary and watershed. *Journal of Coastal Research* 32:3-12.

Kennish, M.J., Roche, M.B. & T.R. Tatham. 1984. Anthropogenic effects on aquatic communities. Pages 318-337 in Kennish, M.J. and R.A. Lutz (eds). *Lecture Notes on Coastal and estuarine studies. Ecology of Barnegat Bay*, New Jersey. New York, Springer Verlag

Kennish, M.J. et al. 2007. Barnegat Bay-Little Egg Harbor estuary: Case study of a highly eutrophic coastal bay system. *Ecological Applications* 17 (supplement): S3-S17.

Kolker A.S., Goodbred Jr S.L., Hameed S. & Cochran J.K. 2009. High-resolution records of the response of coastal wetland systems to long-term and short-term sea-level variability. Estuarine, Coastal and Shelf Science 84: 493-508.

Lake, J.L., R.A. McKinney, F.A. Osterman, R.J. Pruell, J. Kiddon, S.A. Ryba & A.D. Libby. 2001. Stable nitrogen isotopes as indicators of anthropogenic activities in small freshwater systems. *Can. J. Fish. Aquatic Sci*. 58: 870-878.

Lathrop, R.G. 2004. Measuring land use change in New Jersey: land use update to year 2000. Rutgers University, Grant F. Walton Center for Remote Sensing and Spatial Analysis, New Brunswick, NJ, CRSSA Report#2007-04.

Lathrop, R.G. & Haag, S. 2007. Assessment of Land Use Change and Riparian Zone Status in the Barnegat Bay and Little Egg Harbor Watershed: 1995-2002-2006. Rutgers University, Grant F. Walton Center for Remote Sensing and Spatial Analysis, New Brunswick, NJ, CRSSA Report#2007-04.

Litke, D.W. 1999. *Review of Phosphorus Control Measures in the United States and Their Effects on Water Quality*. U.S. Geological Survey, Water Sources Investigations Report 99-4007, National Water Quality Assessment Program, Denver, CO.

Macko, S.A., and N.E. Ostrom. 1994. Pollution studies using stable plankton in a shallow embayment in Northern Puget Sound. Estuarine isotopes. p. 45–62. In K. Lajtha and R. Michener (ed.) Stable isotopes in ecology and environmental science. Blackwell Scientific Publ., Oxford.

Maidment, D. R. and S. Morehouse. 2002. Arc Hydro: GIS for Water Resources, ESRI Press, Redlands, Ca.

McAndrews, J. H., Berti, A. A., and Norris, G. (1973). "Key to the Quaternary Pollen and spores of the Great Lakes Region." Royal Ontario Museum, Toronto.

McClelland, J.W., and I. Valiela. 1998. Linking nitrogen in estuarine producers to land-derived sources. *Limnol. Oceanogr*. 43:577–585.

McClelland, J.W., I. Valiela, and R.H. Michener. 1997. Nitrogen-stable isotope signatures in estuarine food webs: A record of increasing urbanization in coastal watersheds. *Limnol. Oceanogr*. 42:930–937.

Moore P, Webb J, Collinson M (1989) Pollen Analysis. Blackwell, Oxford.

Moreno-Garrido, I., Lubián, L.M., Jiménez, B., Soares, A.M.V.M. & Blasco, J. 2007. Estuarine sediment toxicity tests on diatoms: sensitivity comparison for three species. Estuarine, Coastal and Shelf Science 71: 278-286.

Mountford, K., 1971. *Plankton studies in Barnegat Bay*. Ph.D. thesis, Rutgers University, New Brunswick, New Jersey.

Olsen, P.S. & J.B. Mahoney. 2001. Phytoplankton in the Barnegat Bay-Little Egg Harbor estuarine system: Species composition and picoplankton bloom development. *Journal of Coastal Research*, special issue 32: 115-143.

Potapova, M. and D.F. Charles. 2007. Diatom metrics for monitoring eutrophication in rivers of the United States. *Ecological Indicators.* 7: 48-70.

Potapova, M., Desianti, N., Velinsky, D. & Mead, J. 2013. Barnegat Bay nutrient inference model. Final Report submitted to New Jersey Department of Environmental Protection (Trenton, NJ).

Punt W. et al. 1976-2009. The Northwest European Pollen Flora, I-IX. Elsevier, Amsterdam

Reavie, E.D., Axler, R.P., Sgro, G.V., Danz, N.P., Kingston, J.C., Kireta, A.R., Brown, T.N., Hollenhorst, T.P., and Ferguson, M.J. 2006. Diatom-based weighted-averaging transfer functions for Great Lakes coastal water quality: relationships to watershed characteristics. *Great Lakes Research* 32: 321-347.

Reille, M. 1992-98. *Pollen et spores d'Europe et d'Afrique du Nord*. Laboratoire de Botanique Histoque et Palynologie.

Ritchie J.C., McHenry J.R. 1990. Application of radioactive fallout Cesium-137 for measuring soil-erosion and sediment accumulation rates and patterns: A review. *Journal of Environmental Quality* 19:215–233.

Ruttenberg, K.C. 1992. Development of a sequential extraction method for different forms of phosphorus in marine sediments. *Limnology and Oceanogr*aphy 37: 1460-1482.

Sawai, Y., Horton, B.P., and Nagumo, T. 2004. Diatom-based elevation transfer function along the Pacific coast of eastern Hokkaido, northern Japan – an aid in paleo-seismic study along the coasts near Kurile subduction zone. *Quaternary Sciemce Reviews* 23: 2467-2483.

Schelske, C.L. & Hodell, D.A. 1991. Recent changes in productivity and climate of Lake Ontario detected by isotopic analysis of sediments. *Limnol. Oceanogr*. 36: 961-975.

Schelske, C.L. & Hodell, D.A. 1995. Using carbon isotopes of bulk sedimentary organic matter to reconstruct the history of nutrient loading and eutrophication in Lake Erie. *Limnol. Oceanogr*. 40: 918-929.

Seitzinger, S.P., Styles, R.M. and Pilling, I.E. 2001. Benthic Microalgal and Phytoplankton Production in Barnegat Bay, New Jersey (USA): Microcosm Experiments and Data Synthesis. *Journal of Coastal Research* 32: 144-162.

Shaffer, G.P. and Sullivan, M.J. 1988. Water column productivity attributable to displacd benthic diatoms in well-mixed shallow estuaries. *Journal of Phycology* 24: 132-140.

Short, S.K., Elias, S.A., Waythomas, C.F., and Williams, N.E., 1992. Fossil Pollen and Insect Evidance for Postglacial Enviromental conditions, Nushgak and Holitna Lowland Regions, Southwest Alaska. *Artic* 45: 381-392.

Smith, V.H. 2006. Responses of estuarine and costal marine phytoplankton to nitrogen and phosphorus enrichment. *Limnology and Oceanography* 51: 377-384.

Snoejis, P. (ed.) 1993. Intercalibration and distribution of diatom species in the Baltic Sea. I. Opulus press, Uppsala, 130pp.

Snoejis, P. & Balashova, N. (eds.) 1998. Intercalibration and distribution of diatom species in the Baltic Sea. V. Opulus press, Uppsala, 144 pp.

Snoeijs, P. & Kasperoviçiené, J. (eds.) 1996. Intercalibration and distribution of diatom species in the Baltic Sea. IV. Opulus press, Uppsala, 126 pp.

Snoeijs, P. & Potapova, M. (eds.) 1995. Intercalibration and distribution of diatom species in the Baltic Sea. III. Opulus press, Uppsala, 126 pp.

Snoejis, P. & Vilbaste, S. (eds.) 1994*:* Intercalibration and distribution of diatom species in the Baltic Sea, II. Opulus press, Uppsala,125 pp.

Sullivan, M.J. 1975. Diatom communities from a Delaware salt marsh. *Journal of Phycology.* 11: 384–90.

Sullivan, M.J. & Currin, C.A. 2000. Community structure and functional dynamics of benthic microalgae in salt marshes. Pages 81–106 i*n* Weinstein, M.P. and D.A. Kreeger, eds. *Concepts and Controversies in Tidal Marsh Ecology.* Kluwer Academic Publishers. Dordrecht, NE.

Swackhamer, D.L. 1987. Quality Assurance Plan for Green Bay Mass Balance Study - PCBs and Dieldrin, U.S .Environmental Protection Agency, Great Lakes National Program Office, 1987.

Ter Braak, C. J. F., & Smilauer, P. 2012. CANOCO Reference Manual and User's Guide: Software for Ordination (version 5.0). Biometris, Wageningen and Ceske Budejovice. 496 pp.

Tinner, W. & Hu, F.S. 2003. Size parameters, size-class distribution, and area-number relationship of microscopic charcoal: relevance for fire reconstruction. *The Holocene* 13: 499-505.

Trobajo, R. & Sullivan, M. 2010. Applied diatom studies in estuaries and shallow coastal environments. Pages 309-323 in Smol, J.P. and Stoermer, E.F. (eds). *The diatoms: appicatios for the environmental and Earth sciences*. Cambridge, Cambridge University Press.

Ulseth, A.J. & Hershey, A.E. 2005. Natural abundances of stable isotopes trace anthropogenic N and C in an urban stream. *Journal North Amer. Benth. Soc.*: 24(2): 270-289.

Underwood, G.J.C. 2000. Changes in microalgal species composition, biostabilisation potential and succession during saltmarsh restoration, Pages 143-154 in: Sherwood, B.R. et al. (eds). *British Salt Marshes*. Cardigan, Linnean Society of London/Forrest Text.

U.S. EPA 1993. Methods for the determination of chemical substances in marine and estuarine environmental samples. Environmental Monitoring Systems Laboratory, Office of Research and Development, U.S. Environmental Protection Agency, Report EPA-600/R-92/121.

US EPA 1997. Methods for the Determination of Chemical Substances in Marine and Estuarine Environmental Matrices. 2nd edition. September 1997. (NSCEP or NTIS / PB97-127326).

US EPA 2005. National Coastal Condition Report II (NCCR II). (http://water.epa.gov/type/oceb/2005_downloads.cfm)

Valette-Silver, N.J. 1993. The use of sediment cores to reconstruct historical trends in contamination of estuarine and coastal sediments. *Estuaries.* 16: 577-588.

van Geel, B. &Aptroot, A. 2006. Fossil ascomycetes in Quaternary deposits. Nova Hedwigia 82, 313-329.

van Geel, B., Coope, G.R. & van der Hammen, T. 1989. Palaeoecology and stratigraphy of the Late glacial type section at Usselo (the Netherlands). *Review of Palaeobotany and Palynology* 60: 25-129.

Varela, M. and Penas, E. 1985. Primary production of benthic microalgae in an intertidal sand flat of the Ria de Arosa, NW Spain. *Marine Ecology Progress Series* 25: 111-119.

Velinsky, D.J., Charles, D.F. and Ashley, J. 2007. Contaminant Sediment Profiles of the St. Jones River Marsh, Delaware: A Historical Analysis. Final Report submitted to DNREC. PCER Report No. 07-05. The Academy of Natural Sciences, Patrick Center for Environmental Research, Philadelphia, PA.

Velinsky, D.J., C. Sommerfield and D. Charles. 2010a. Vertical profiles of radioisotopes, contaminants, nutrients and diatoms in sediment cores from the tidal Christina River Basin: A historical analysis. Report submitted to Dr. R. Greene (DNREC; Division of Water Resources; State of Delaware, Dover DE). Patrick Center Report 09-02, The Academy of Natural Sciences, Philadelphia, PA.

Velinsky, D.J., C. Sommerfield and D. Charles. 2010b. Vertical Profiles of Radioisotopes, Nutrients and Diatoms in Sediment Cores from the Tidal Murderkill River Basin: A Historical Analysis of Ecological Change and Sediment Accretion. PCER Report No. 10-01; Final Report

submitted to Delaware Department of Natural Resources and Environmental Control (Dover, DE).

Velinsky, D.J., Sommerfield, C., Enache, M. and Charles, D. 2010c. Nutrient and ecological histories in Barnegat Bay, New Jersey. Final Report submitted to New Jersey Department of Environmental Protection (Trenton, NJ).

Vos, P. C. and DeWolf, H. 1993. Diatoms as a Tool for Reconstructing Sedimentary Environments in Coastal Wetlands - Methodological Aspects. *Hydrobiologia* 269/270, 285-296.

Wekstrom, K. 2006. Assessing recent eutrophication in coastal waters of the Gulf of Finland (Baltic Sea) using subfossil diatoms. *Journal of Paleolimnology* 35:571-592.

Wieben, C.M., Baker, R.J., and Nicholson, R.S., 2013. Nutrient concentrations in surface water and groundwater, and nitrate source identification using stable isotope analysis, in the Barnegat Bay-Little Egg Harbor watershed, New Jersey, 2010–11: U.S. Geological Survey Scientific Investigations Report 2012–5287, 44 p.

Wilderman, C.C. 1984. The floristic composition and distribution patterns of diatom assemblages in the Severn River Estuary, Maryland. Ph.D. thesis. The John Hopkins University, Baltimore, Maryland.

Witkovsky, A., Lange-Bertalot, H. and Metzeltin, D. 2000. Diatom flora of marine coasts. *Iconographia Diatomologica* 7: 1-925.

G) Tables

Table 1. Locations of sediment cores.

Core	Latitude	Longitude
BB-1	40.029883	-74.079950
BB-2	39.847583	-74.147283
BB-3	39.810883	-74.190167
BB-4	39.627361	-74.260222
GB-2	39.513178	-74.413011

Table 2. Rates of sediment accretion for Great Bay Core GB-2 as determined by Cs-137 and 'Constant Rate of Supply' (CRS) and 'Constant Initial Concentration' (CIC) Pb-210 dating methods.

Method	Accretion Rate (cm/yr)
Cs-137	0.52
Pb-210 (CIC)	0.44 ± 0.03
Pb-210 (CRS)	0.47 (0.23-0.92)

Table 3. Bulk sediment properties and radioisotope data for the Great Bay core (GB-2).

Interval cm	CHEM ID ID	Mid-Point cm	% Water	% Solids	Acc. Dry Mass (g cm-2)	Calc Year	Cs-137 uCi/g	Pb-210 uCi/g	Cs-137 +/- (uCi/g)	Pb-210 +/- (uCi/g)	Cs-137 dpm/g	Pb-210 dpm/g
0-1	01509	0.5	49.13	50.87	7.26	2012	2.26E-07	3.55E-06	6.05E-08	7.81E-07	0.502	7.890
1-2	01510	1.5	49.41	50.59	12.70	2010	1.75E-07	4.22E-06	3.24E-08	9.16E-07	0.389	9.363
2-3	01511	2.5	45.04	54.96	22.01	2008	6.27E-08	2.53E-06	4.57E-08	5.56E-07	0.139	5.623
3-4	01512	3.5	46.45	53.55	29.23	2006	1.01E-07	2.92E-06	4.69E-08	6.56E-07	0.225	6.475
4-5	01513	4.5	48.00	52.00	43.23	2004	1.11E-07	2.49E-06	3.03E-08	5.16E-07	0.247	5.533
5-6	01514	5.5	48.81	51.19	60.37	2002	1.29E-07	2.74E-06	3.15E-08	5.56E-07	0.285	6.079
6-7	01515	6.5	51.75	48.25	72.42	2001	1.30E-07	3.60E-06	2.09E-08	7.30E-07	0.290	7.991
7-8	01516	7.5	51.73	48.27	80.99	1999	1.07E-07	3.70E-06	3.93E-08	7.67E-07	0.238	8.213
8-9	01517	8.5	52.82	47.18	86.52	1997	8.70E-08	1.91E-06	1.07E-08	6.19E-07	0.193	4.231
9-10	01518	9.5	52.05	47.95	98.98	1995	2.02E-07	3.61E-06	3.86E-08	7.77E-07	0.447	8.005
10-11	01519	10.5	52.08	47.92	108.66	1993	2.01E-07	4.10E-06	4.57E-08	8.35E-07	0.447	9.091
11-12	01520	11.5	49.15	50.85	118.96	1991	1.35E-07	3.20E-06	7.43E-08	7.32E-07	0.300	7.112
12-13	01521	12.5	46.20	53.80	133.23	1989	2.25E-07	2.55E-06	2.12E-08	5.28E-07	0.500	5.656
13-14	01522	13.5	46.26	53.74	143.25	1987	1.74E-08	3.40E-06	2.80E-07	6.61E-07	0.039	7.551
14-15	01523	14.5	44.88	55.12	155.27	1985	2.77E-07	2.21E-06	1.56E-08	5.97E-07	0.616	4.900
15-17	01524	16	47.40	52.60	194.53	1982	2.19E-07	1.65E-06	1.27E-08	3.32E-07	0.485	3.657
17-19	01525	18	52.69	47.31	239.09	1978	2.85E-07	1.56E-06	1.33E-08	3.98E-07	0.632	3.474
19-21	01526	20	59.13	40.87	270.03	1975	3.41E-07	2.38E-06	1.82E-08	4.69E-07	0.758	5.295
21-23	01527	22	61.79	38.21	303.10	1971	3.32E-07	2.25E-06	1.53E-08	4.94E-07	0.736	4.992
23-25	01528	24	65.18	34.82	333.08	1967	3.09E-07	1.93E-06	1.65E-08	3.90E-07	0.685	4.280
25-27	01529	26	65.52	34.48	360.67	1963	4.16E-07	1.61E-06	1.49E-08	3.12E-07	0.923	3.571
27-29	01530	28	62.68	37.32	396.99	1959	4.02E-07	1.14E-06	1.64E-08	2.43E-07	0.893	2.521
29-31	01531	30	63.27	36.73	424.77	1955	2.37E-07	1.18E-06	1.56E-08	2.59E-07	0.527	2.611
31-33	01532	32	64.67	35.33	457.11	1951	7.57E-08	8.99E-07	6.18E-09	1.77E-07	0.168	1.995
41-43	01537	42	59.62	40.38	621.86	1932	6.91E-09	6.00E-07	2.47E-08	1.81E-07	0.015	1.332
51-53	01542	52	67.16	32.84	785.90	1913	0.00E+00	6.51E-07	0.00E+00	1.63E-07	0.000	1.446
61-63	01547	62	60.35	39.65	968.76	1894	2.35E-09	5.62E-07	9.78E-10	1.40E-07	0.005	1.247
71-73	01552	72	56.58	43.42	1147.92	1875	0.00E+00	5.92E-07	0.00E+00	1.24E-07	0.000	1.314
81-83	01557	82	63.45	36.55	1316.13	1855	0.00E+00	5.65E-07	0.00E+00	1.49E-07	0.000	1.253
91-93	01562	92	58.53	41.47	1495.94	1836	0.00E+00	4.62E-07	0.00E+00	1.18E-07	0.000	1.026

Table 4. Summary of organic carbon, organic contaminants and trace metals/metalloids in samples collected in Barnegat and Great Bays[1]. PAH – polycyclic aromatic hydrocarbons; OCP – organochlorine pesticides; PCB – polychlorinated biphenyls.

Constituent	Units	Mean	Median	Maximum	Minimum	Count
Organic C	Wt%	2.8	1.9	14.6	0.1	54
Total PAH	ng/g dw	1151	785	7284	16	56
Total PCB	ng/g dw	10.7	7.8	89	0.7	56
Arsenic (As)	µg/g dw	9.7	7.4	37.7	0.6	54
Cadmium (Cd)	µg/g dw	0.36	0.32	1.50	0.08	54
Chromium (Cr)	µg/g dw	14.3	15.6	25.4	2.9	54
Copper (Cu)	µg/g dw	12.24	6.1	81.6	1.1	54
Iron (Fe)	µg/g dw	20942	19553	55711	1040	54
Lead (Pb)	µg/g dw	20.6	15.0	89.8	2.9	54
Nickel (Ni)	µg/g dw	4.69	5.22	8.40	0.51	54
Silver (Ag)	µg/g dw	0.28	0.28	0.49	0.08	54
Zinc (Zn)	µg/g dw	84.0	65.9	342.5	8.1	54

[1]Full data are reported in Appendix 1.

Table 5. Sediment Quality Guidelines with Effects Range-Low and Effects Range-Medium for selected polycyclic aromatic hydrocarbons (PAHs), polychlorinated biphenyls (PCBs) and trace elements. [Sediment quality guidelines are from Long et al. (1995). ER-L, Effects Range-Low; ER-M, Effects Range-Medium; mg/kg, micrograms per kilogram; mg/kg, milligrams per kilogram] Table taken from Fischer et al. (in press).

Compound	ER-L	ER-M
PAHs (µg/kg)		
2-Methylnaphthalene	70	670
Acenaphthylene	16	640
Anthracene	85.3	1,100
Benzo (a) anthracene	261	1,600
Benzo (a) pyrene	430	1,600
Chrysene	384	2,800
Dibenz (a,h) anthracene	63.4	260
Fluoranthene	600	5,100
Fluorene	19	540
Naphthalene	160	2,100
Phenanthrene	240	1,500
Pyrene	665	2,600
Total PAHs	4,022	44,792
PCBs (µg/kg)		
Total PCBs	22.7	180
Trace elements (mg/kg)		
Arsenic	8.2	70
Cadmium	1.2	9.6
Chromium	81	370
Copper	34	270
Lead	46.7	218
Mercury	0.15	0.71
Nickel	20.9	51.6
Silver	1	3.7
Zinc	150	410

Table 6. Various parameters for Great Bay core (GB-2).

Interval	CHEM ID	Mid-Point	Age Model[1]	OC	TN	TP	$d^{13}C$	$d^{15}N$	C to N
cm	ID	cm	yr	wt %	wt %	wt %	‰	‰	Molar
0-1	01509	0.5	2012	4.30	0.52	0.089	-17.02	4.26	9.5
1-2	01510	1.5	2010	4.21	0.47	0.080	-17.09	4.30	10.4
2-3	01511	2.5	2008	3.41	0.35	0.081	-17.65	4.29	11.3
4-5	01513	4.5	2004	3.83	0.37	0.067	-17.55	4.18	12.0
6-7	01515	6.5	2001	4.45	0.39	0.062	-17.61	4.21	13.3
8-9	01517	8.5	1997	3.93	0.38	0.062	-17.80	4.10	12.1
10-11	01519	10.5	1993	3.65	0.36	0.063	-18.18	4.42	11.7
12-13	01521	12.5	1989	3.00	0.29	0.060	-18.42	4.13	12.2
14-15	01523	14.5	1985	2.79	0.26	0.060	-18.32	3.73	12.4
17-19	01525	18	1978	3.63	0.33	0.065	-18.07	3.87	12.7
21-23	01527	22	1971	5.22	0.46	0.073	-17.50	3.93	13.2
25-27	01529	26	1963	6.44	0.51	0.070	-17.47	4.25	14.8
29-31	01531	30	1955	5.17	0.39	0.070	-17.84	4.59	15.3
37-39	01535	38	1940	5.91	0.45	0.060	-17.43	4.08	15.2
45-47	01539	46	1925	4.53	0.41	0.068	-17.75	3.36	12.9
53-55	01543	54	1909	5.89	0.55	0.067	-16.99	2.64	12.6
61-63	01547	62	1894	4.57	0.40	0.063	-17.64	2.92	13.2
69-71	01551	70	1878	3.60	0.31	0.061	-17.60	3.79	13.6
77-79	01555	78	1863	4.35	0.37	0.061	-17.27	2.80	13.6
85-87	01559	86	1848	4.00	0.36	0.071	-17.51	2.79	12.8
93-95	01563	94	1832	3.03	0.30	0.065	-17.34	1.95	11.7

Note: dates are based on the Cs-137 derived rate of 0.52 cm/yr.

Table 7. Strength of the relationships between diatom assemblage composition and environmental variables as measured by the significance of the first CCA axes. Bold: significant at p=0.002. CCAs with species dataset that included only species that reached 1% relative abundance in at least 5 samples.

Environmental variable	All 100 sites		34 marsh sites		66 open-water sites	
	F-ratio	P-value	F-ratio	P-value	F-ratio	P-value
Marsh/Open site	**5.5**	**0.001**				
Depth, m	**4.8**	**0.001**	2.6	0.004	1.5	0.056
Dissolved Oxygen, mg/L	**2.6**	**0.001**	1.3	0.141	**3.6**	**0.001**
pH	**2.5**	**0.001**	2.1	0.005	1.4	0.077
Salinity, psu	**9.6**	**0.001**	**4.2**	**0.001**	**7.5**	**0.001**
Turbidity	**2.8**	**0.001**	1.3	0.110	1.4	0.127
Total Suspended Solids, mg/L	1.6	0.022	0.8	0.692	1.3	0.124
Chlorophyll A, Log µg/L	**5.4**	**0.001**	1.7	0.027	**5.5**	**0.001**
Particulate Phosphorus, Log µg P/L	**3.7**	**0.001**	1.3	0.101	**4.2**	**0.001**
Total Dissolved Phosphorus, Log µg P/L	**8.4**	**0.001**	**4.3**	**0.001**	**5.8**	**0.001**
Total Phosphorus, Log µg P/L	**3.3**	**0.001**	1.8	0.010	**2.4**	**0.001**
Ammonia, Log µg N/L	**3.8**	**0.001**	1.0	0.426	**4.2**	**0.001**
Nitrate + Nitrite, Log µg N/L	**3.6**	**0.001**	**2.6**	**0.001**	2.5	0.002
Total Kjeldahl Nitrogen, µg N/L	2.0	0.010	1.3	0.172	1.4	0.101
Total Inorganic Nitrogen, µg N/L	2.3	0.004	1.4	0.078	**2.2**	**0.001**
Total Nitrogen, µm N/L	2.1	0.007	1.3	0.127	1.4	0.078
Carbon sediment, Log µg/g	**5.2**	**0.001**	**2.3**	**0.001**	**3.1**	**0.001**
Nitrogen sediment, Log µg/g	**5.4**	**0.001**	2.3	0.002	2.5	0.002
Phosphorus sediment, Log µg/g	**3.1**	**0.001**	0.9	0.553	**2.5**	**0.001**
"Developed" land-use, sqrt %	**5.2**	**0.001**	2.4	0.002	**4.0**	**0.001**
"Forest" land-use, sqrt %	1.6	0.041	1.2	0.192	1.6	0.026
"Grassland" land-use, sqrt %	1.0	0.404	1.1	0.338	1.0	0.484
"Wetland" land-use, sqrt %	**2.9**	**0.001**	1.7	0.023	2.2	0.004
"Agricultural" land-use, sqrt %	1.6	0.043	0.7	0.835	1.8	0.014
"Undeveloped" land-use, sqrt %	**4.9**	**0.001**	**2.2**	**0.003**	**3.7**	**0.001**
"Developed+agricultural" land-use, sqrt %	**5.0**	**0.001**	2.4	0.002	**3.8**	**0.001**

Table 8. Strength of the relationships between diatom assemblage composition and environmental variables with effect of salinity partialled out, as measured by the significance of the first CCA axes. Bold: significant at p=0.002. CCAs with species dataset that included only species that reached 1% relative abundance in at least 5 samples.

Environmental variable	All 100 sites		34 marsh sites		66 open-water sites	
	F-ratio	P-value	F-ratio	P-value	F-ratio	P-value
Marsh/Open site	**6.0**	**0.001**				
Depth	**5.3**	**0.001**	1.5	0.064	1.6	0.029
Dissolved Oxygen, mg/L	1.4	0.076	1.5	0.065	1.6	0.036
Turbidity	3.1	0.002	1.4	0.059	1.5	0.058
Chlorophyll A, Log µg/L	**2.5**	**0.001**	1.2	0.217	**2.5**	**0.001**
Particulate Phosphorus, Log µg P/L	2.4	0.002	1.3	0.100	1.8	0.015
Total Dissolved Phosphorus, Log µg P/L	**3.5**	**0.001**	2.2	0.002	**2.7**	**0.001**
Total Phosphorus, Log µg P/L	**3.1**	**0.001**	1.5	0.022	**2.4**	**0.001**
Ammonia, Log µg N/L	2.0	0.006	1.1	0.248	1.7	0.018
Nitrate + Nitrite, Log µg N/L	2.5	0.004	1.5	0.033	2.2	0.005
Total Inorganic Nitrogen, µg N/L	2.3	0.002	1.6	0.018	1.8	0.022
Carbon sediment, Log µg/g	**4.2**	**0.001**	1.1	0.259	1.6	0.025
Nitrogen sediment, Log µg/g	**4.7**	**0.001**	1.3	0.154	2.3	0.005
Phosphorus sediment, Log µg/g	**3.3**	**0.001**	1.0	0.395	**2.7**	**0.001**
"Developed" land-use, sqrt %	**2.5**	**0.001**	1.4	0.059	2.1	0.004
"Wetland" land-use, sqrt %	1.5	0.046	1.3	0.130	1.2	0.162
"Undeveloped" land-use, sqrt %	2.0	0.006	1.0	0.408	1.6	0.045
"Developed+agricultural" land-use, sqrt %	2.2	0.003	1.3	0.093	1.8	0.019

Table 9. Performance of diatom inference models as estimated by R^2_{boot} value. Values equal or greater than 0.5 are in bold. WA -Weighed Averaging model, WA-PLS - Weighed Averaging- Partial Least Squares model, ML- Maximum Likelihood model, MAT- Modern Analog Technique model.

Dataset/Variable	WA		WA-PLS	ML	MAT
	Inverse	Classic			
Depth	0.36	0.36	0.39	0.42	0.40
Salinity, psu	**0.75**	**0.76**	**0.81**	**0.79**	**0.78**
Chlorophyll A, Log μg/L	**0.51**	**0.51**	**0.61**	**0.59**	**0.50**
Total Dissolved Phosphorus, Log μg P/L	**0.64**	**0.64**	**0.69**	**0.69**	**0.71**
Total Phosphorus, Log μg P/L	0.24	0.25	0.28	0.29	0.26
Particulate Phosphorus, Log μg P/L	0.28	0.29	0.38	0.36	0.25
Carbon sediment, Log μg/g	0.44	0.44	**0.51**	0.41	0.36
Nitrogen sediment, Log μg/g	0.48	0.49	**0.54**	0.49	**0.50**
Phosphorus sediment, Log μg/g	0.33	0.33	0.37	0.35	0.31
"Developed" land-use, sqrt %	0.39	0.39	0.38	0.43	0.39

Table 10. Conditional (marginal) and joint effects of environmental variables on diatom assemblage composition based on variance partition analysis.

Variables	% explained variance	% of all variance
Salinity and Chlorophyll A	100.0	6.5
Salinity	53.6	3.5
Chlorophyll A	17.4	1.1
Joint	29.0	1.9
Salinity and TDP	100.0	6.7
Salinity	34.3	2.3
TDP	20.8	1.4
Joint	44.9	3.0

Table 11. List of diatom taxa associated with low concentrations of sediment contaminants.

Actinoptychus senarius (Ehrenberg) Ehrenberg
Amphora allanta Hohn & Hellerman
Amphora pediculus (Kützing) Grunow in Schmidt et al.
Biddulphia pulchella S.F. Gray
Brockmaniella brockmannii (Hustedt) Hasle, von Stosch & Syvertsen
Chamaepinnularia sp. 1 COAST
Cocconeis convexa Giffen
Cocconeis placentula var. euglypta (Ehrenberg) Grunow
Delphineis minutissima (Hustedt) Simonsen
Dimeregramma minor (Gregory) Ralfs in Pritchard
Diploneis bombus Cleve-Euler in Backman & Cleve-Euler Backman
Diploneis stroemii Hustedt
Eunotogramma sp. 1 COAST
Fallacia litoricola (Hustedt) Mann in Round, Crawford & Mann
Grammatophora angulosa Ehrenberg
Grammatophora oceanica Ehrenberg
Gyrosigma fasciola (Ehrenberg) Griffith & Henfrey
Gyrosigma macrum (W. Smith) Griffith & Henfrey
Gyrosigma tenuissimum (W. Smith) Griffith & Henfrey
Hyalodiscus scoticus (Kützing) Grunow
Melosira nummuloides (Dillwyn) Agardh
Navicula directa (W. Smith) Brébisson
Navicula sp. 106 COAST
Navicula sp. 106 COAST
Navicula transistantioides Foged
Navicula vandamii Schoeman & Archibald
Nitzschia coarctata Grunow
Nitzschia distans var. distans Gregory
Nitzschia laevis Hustedt
Nitzschia reversa W. Smith
Nitzschia sigma (Kützing) W. Smith
Odontella aurita Agardh
Pleurosigma elongatum W. Smith
Pleurosigma salinarum (Grunow) Grunow in Cleve & Grunow
Rhabdonema adriaticum Kützing
Seminavis sp. 1 COAST
Skeletonema spp
Tabularia cf. waernii
Thalassionema nitzschioides (Grunow) Van Heurck
Thalassiosira cedarkeyensis Prasad in Prasad, Fryxell & Livingston
Thalassiosira cf. oestrupii
Thalassiosira eccentrica (Ehrenberg) Cleve emend Fryxell & Hasle
Thalassiosira levanderi Van Goor
Thalassiosira proschkinae Makarova in Makarova, Genkal & Kuzmin
Thalassiosira weissflogii (Grunow) G. Fryxell & Hasle
Tryblionella apiculata Gregory
Tryblionella levidensis W. Smith
Tryblionella sp. 1 COAST

Table 12. List of diatom taxa associated with relatively high concentrations of sediment contaminants.

Achnanthidium capitatum Riaux Gobin, Romero, Compère & Al Handal
Achnanthidium flexuistriatum C. Riaux-Gobin, P. Compère & A. Witkowski
Adlafia sp. 4 COAST
Amphora adumbrata Hohn & Hellerman
Amphora lineolata Ehrenberg
Amphora sp. 1 COAST
Amphora sp. 3 COAST
Amphora sp. 6 COAST
Amphora sublaevis Hustedt
Anorthoneis vortex Sterrenburg
Astartiella bremeyeri (Lange-Bertalot) Witkowski & Lange-Bertalot
Biremis lucens (Hustedt) Sabbe, Witkowski & Vyverman
Cocconeis placentula var. lineata (Ehrenberg) Van Heurck
Fallacia amphipleuroides (Hustedt) Mann
Fallacia pygmaea (Kützing) Stickle & Mann
Fragilaria gedanensis Witkowski
Fragilaria sp. 1 COAST
Halamphora aponina (Kützing) Z. Levkov
Navicula arenaria Donkin
Navicula cf. microcari
Navicula cf. veneta
Navicula cincta (Ehrenberg) Ralfs
Navicula gregaria Donkin
Navicula jonssonii Østrup
Navicula normalis Hustedt
Navicula phyllepta kützing Kützing
Navicula salinicola Hustedt
Navicula sp. 105 COAST
Navicula sp. 2 COAST
Navicula sp. 29 COAST
Navicula sp. 39 COAST
Navicula sp. 41 COAST
Navicula sp. 43 COAST
Navicula sp. 63 COAST
Navicula sp. 66 COAST
Nitzschia closterium (Ehrenberg) W. Smith
Nitzschia scalpelliformis Grunow in Cleve & Grunow
Nitzschia thermaloides Hustedt
Opephora sp. 1 COAST
Opephora sp. 4 COAST
Pierrecomperia catenuloides K. Sabbe, W. Vyverman & L. Ribeiro
Planothidium sp. 11 COAST
Pseudostaurosira perminuta (Grunow) Sabbe & Vyverman
Pseudostaurosira sopotensis Witkowski & Lange-Bertalot
Rhopalodia musculus (Kützing) Otto Müller
Seminavis pusilla (Grunow) E.J. Cox & G. Reid
Stauroforma atomus Hustedt
Stauroforma exiguiformis (Lange-Bertalot) Flower, Jones & Round

H) Figures

Figure 1. Location of 50 sites sampled in 2012 where sediment contaminants were analyzed and PAHs distribution. Diameter of the circles corresponds to relative concentration of PAHs.

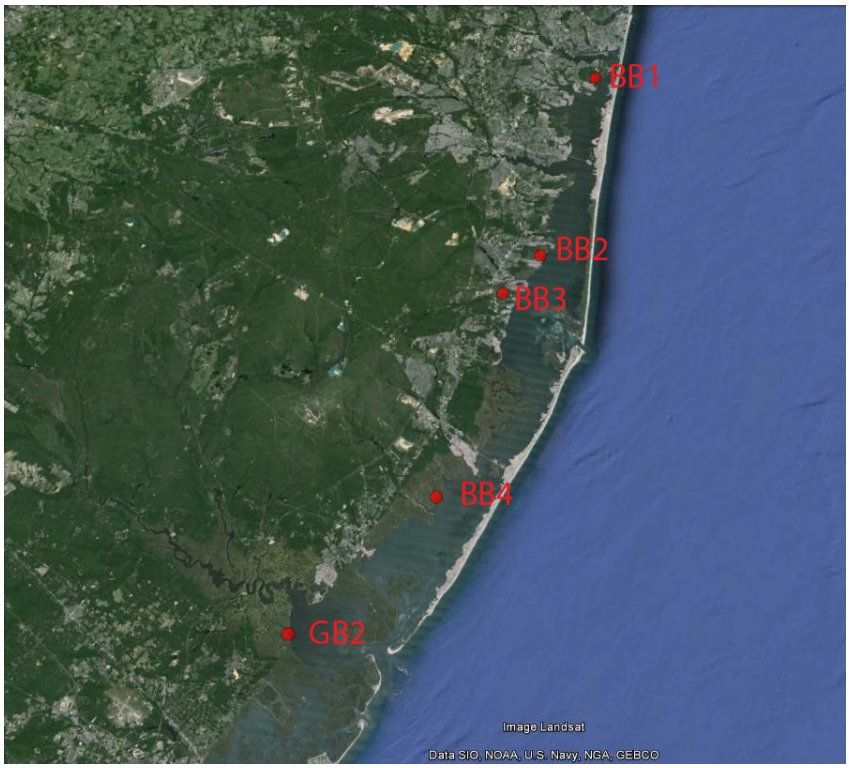

Figure 2. Locations of sediment cores collected in 2009 (BBO cores) and 2014 (GB-2).

Figure 3. Location of core GB-2 collected May 22, 2014.

Figure 4. Collecting sediment core GB-2.

Figure 5. Extruding and sectioning the core GB-2.

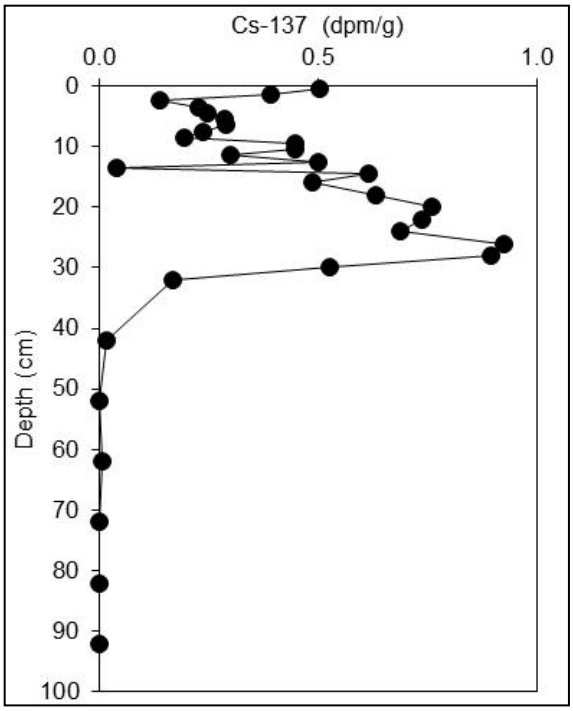

Figure 6. Depth profile of Cs-137 activities in Great Bay Core GB-2.

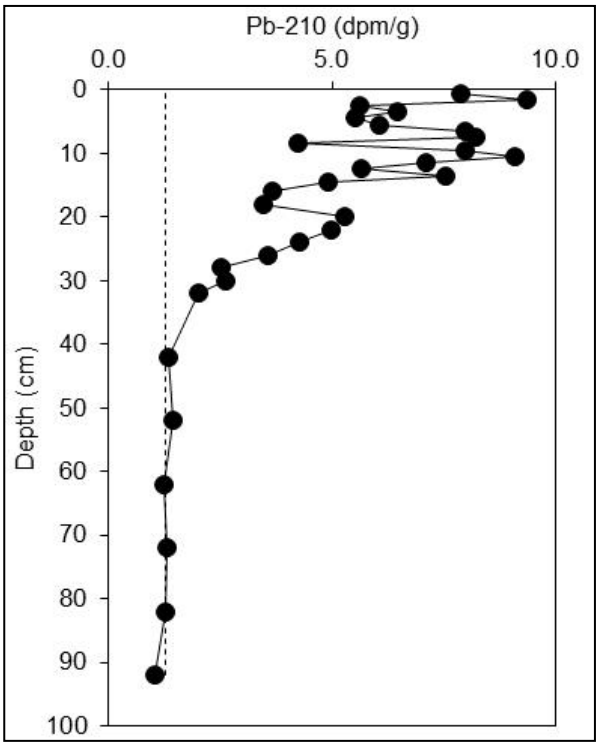

Figure 7. Depth profile of Pb-210 activities in Great Bay Core GB-2. The 'supported' Pb-210 activity is shown by the vertical dashed line.

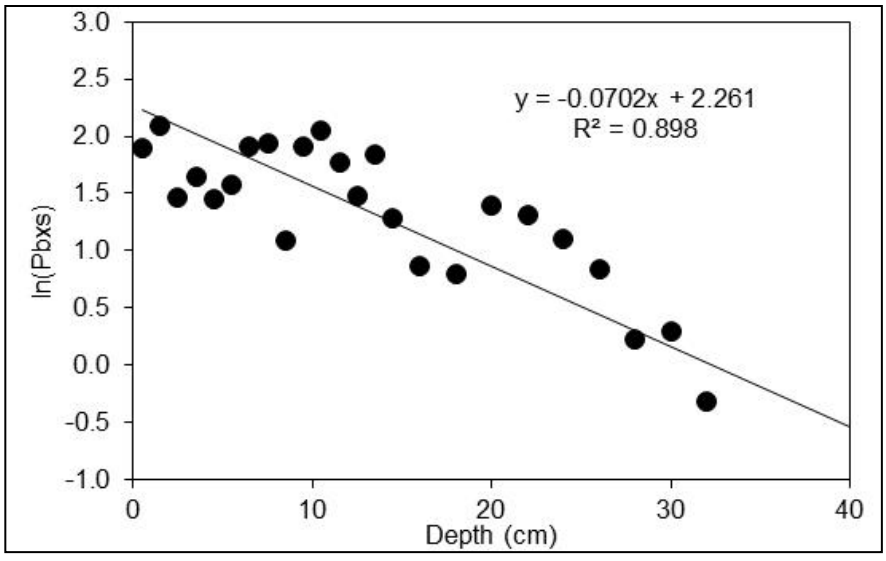

Figure 8. Natural log of excess Pb-210 activity plotted against depth in the GB-2 sediment core used in the CIC accretion rate calculation.

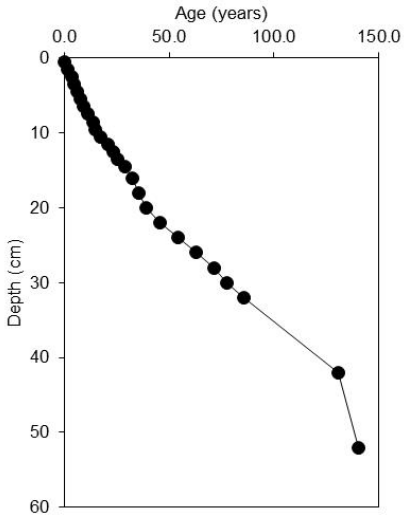

Figure 9. Depth-specific age of sediment in core GB-2 using the CRS model.

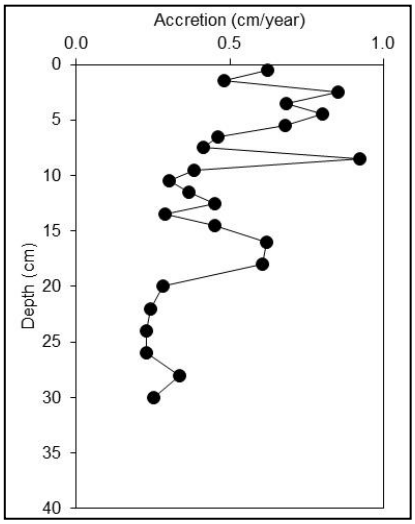

Figure 10. Depth-specific accretion rate in core GB-2.

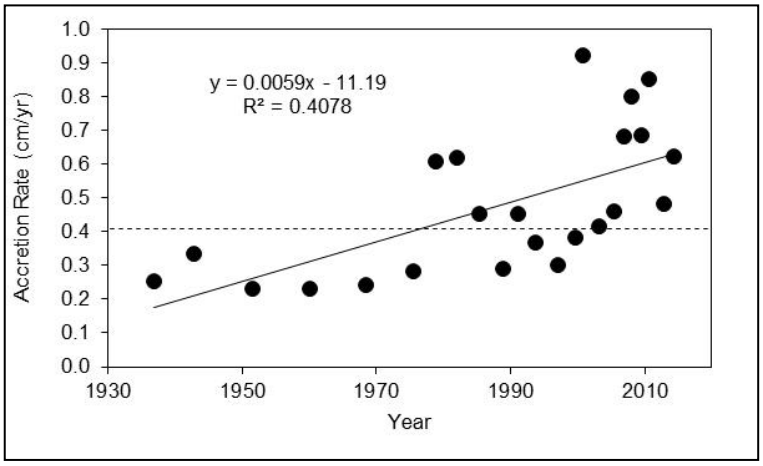

Figure11. Depth-specific accretion rates over time at site GB-2. The average rate of sea-level rise at Atlantic City, NJ is denoted by the dashed line.

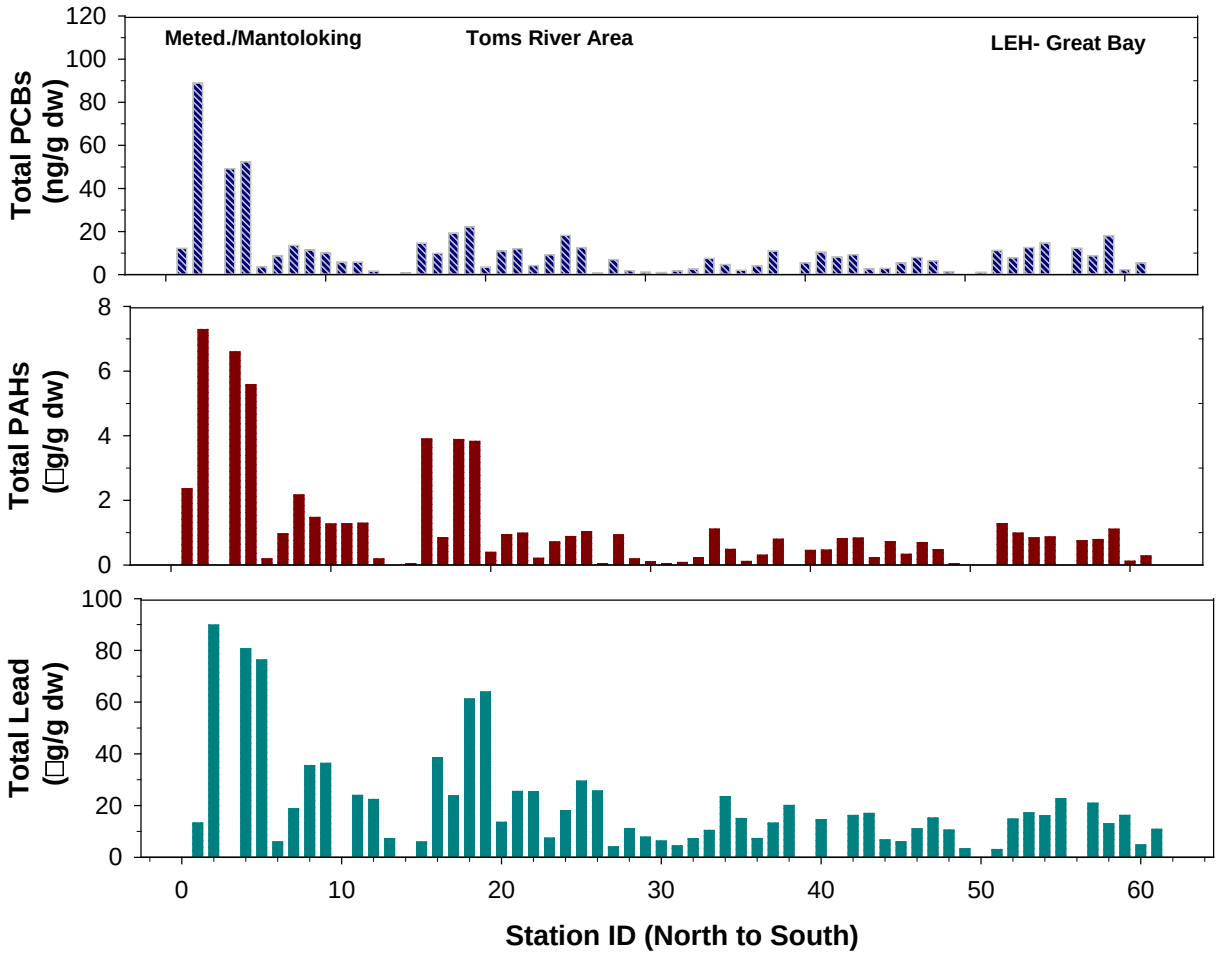

Figure 12. Concentrations of selected contaminants in Barnegat and Great Bays. Concentrations are presented from North to South (see Appendix 1 for actual locations).

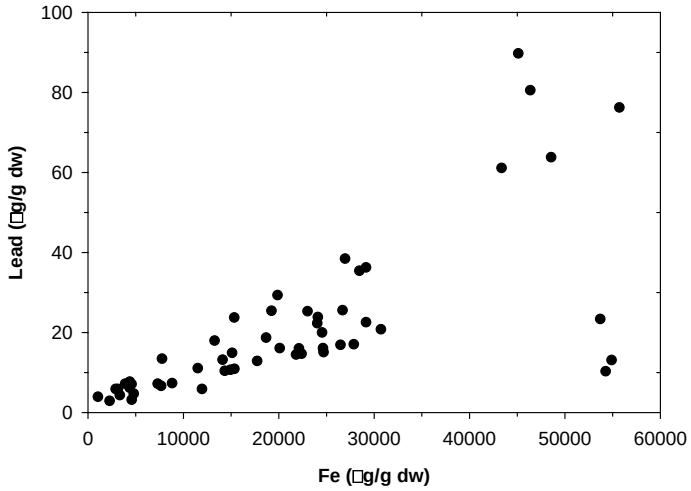

Figure 13. Relationship between iron and lead in the sediments of Barnegat and Great Bays.

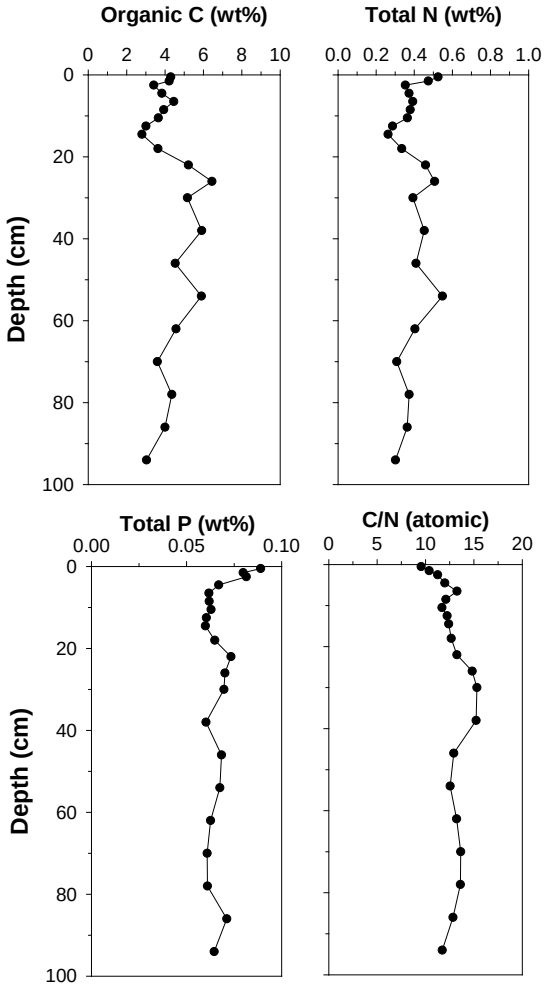

Figure 14. Concentrations with depth for organic carbon, total nitrogen and phosphorus and the carbon to nitrogen ratio (molar) for the Great Bay core.

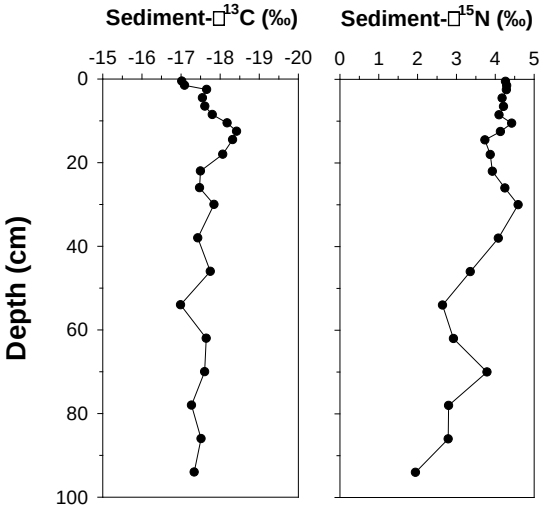

Figure 15. The stable isotopic compositions of C and N with depth from the Great Bay core.

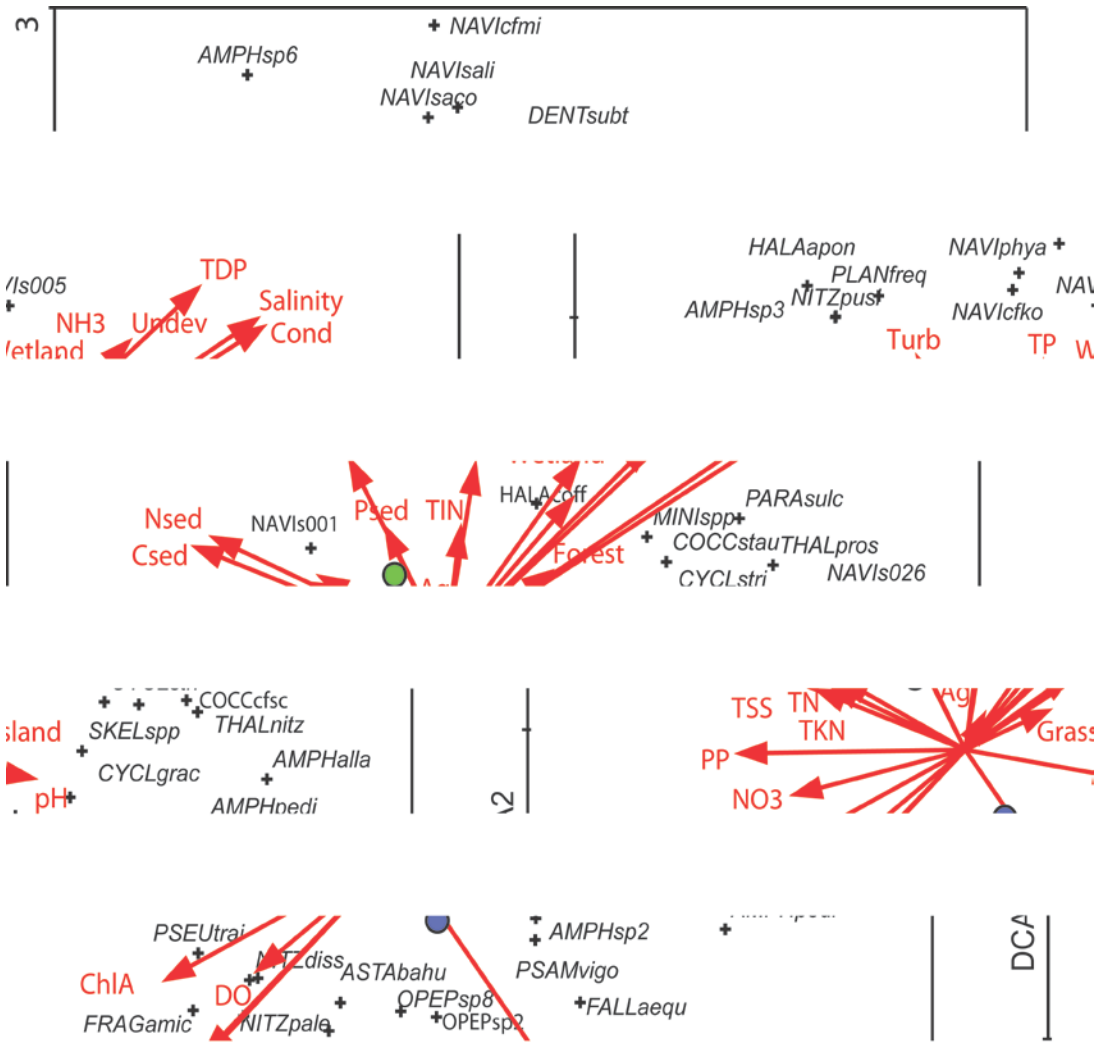

Figure 16. Biplot of species and environmental variables showing the result of a DCA exploring relationships between diatom assemblages and water-quality and land-use parameters, dataset of 100 sites from the Barnegat and Great Bays. Only centroids for species with highest weights (20-100%) are shown. Species short codes correspond to those in Appendix 2. Green circle is the centroid of marsh sites and blue circle is the centroid of open-water sites.

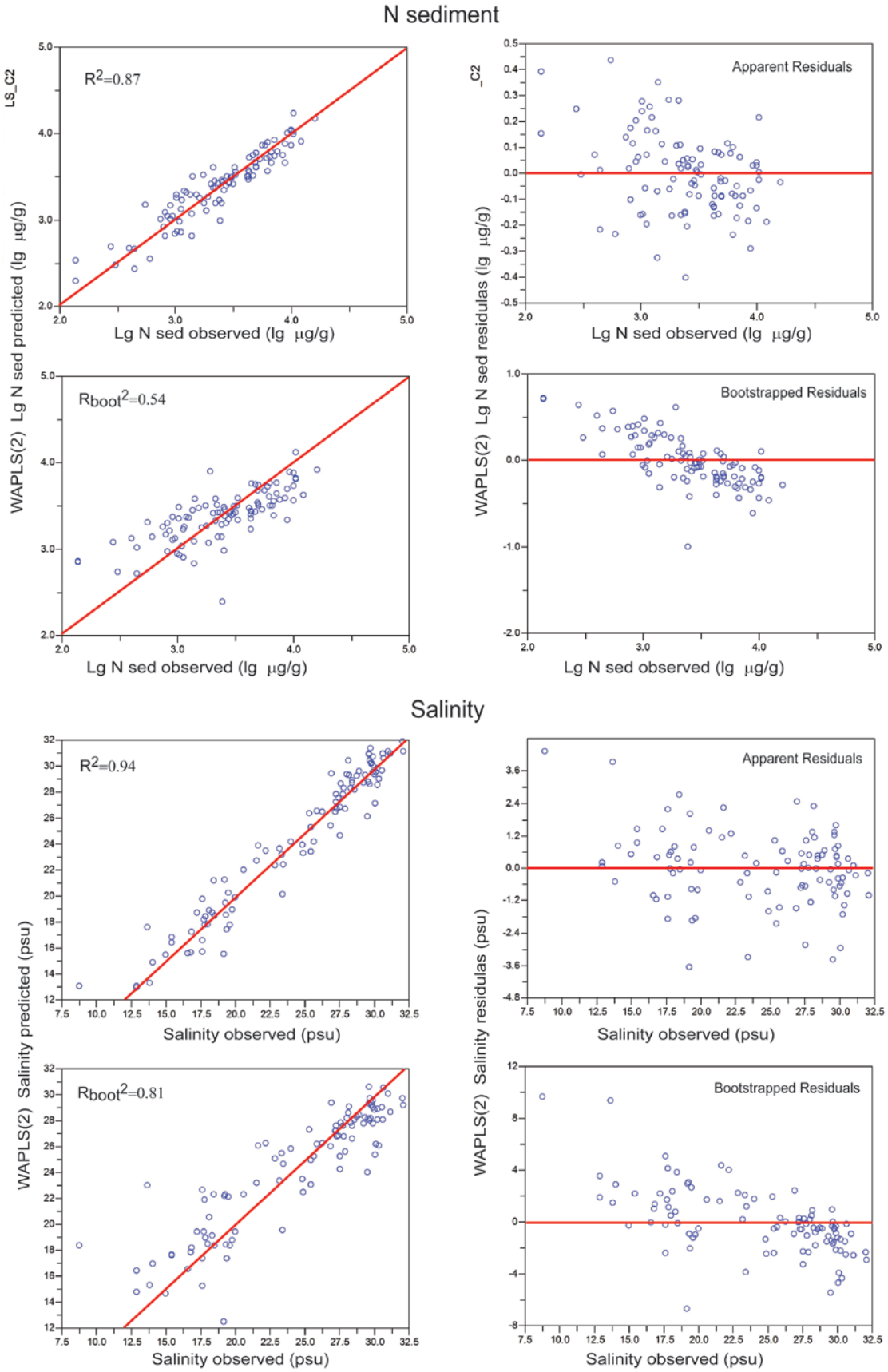

Figure 17. Performance of WAPLS inference models for N sediment and Salinity.

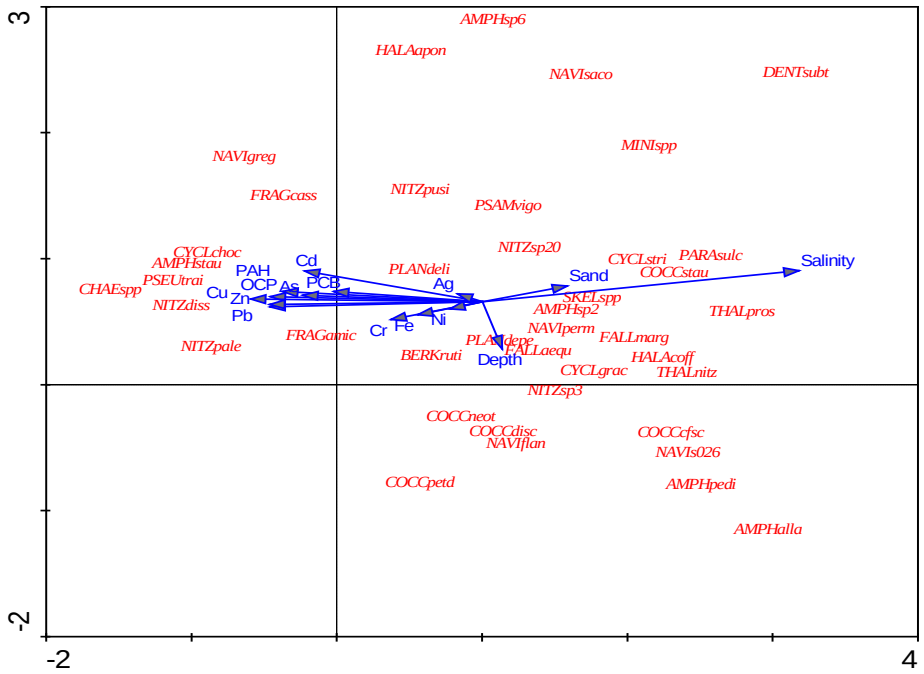

Figure 18. Biplot of species and environmental variables showing the result of a DCA exploring relationships between diatom assemblages and sediment contaminants, dataset of 50 sites from the Barnegat and Great Bays. Only centroids for species with highest weights (20-100%) are shown. Species short codes correspond to those in Appendix 2.

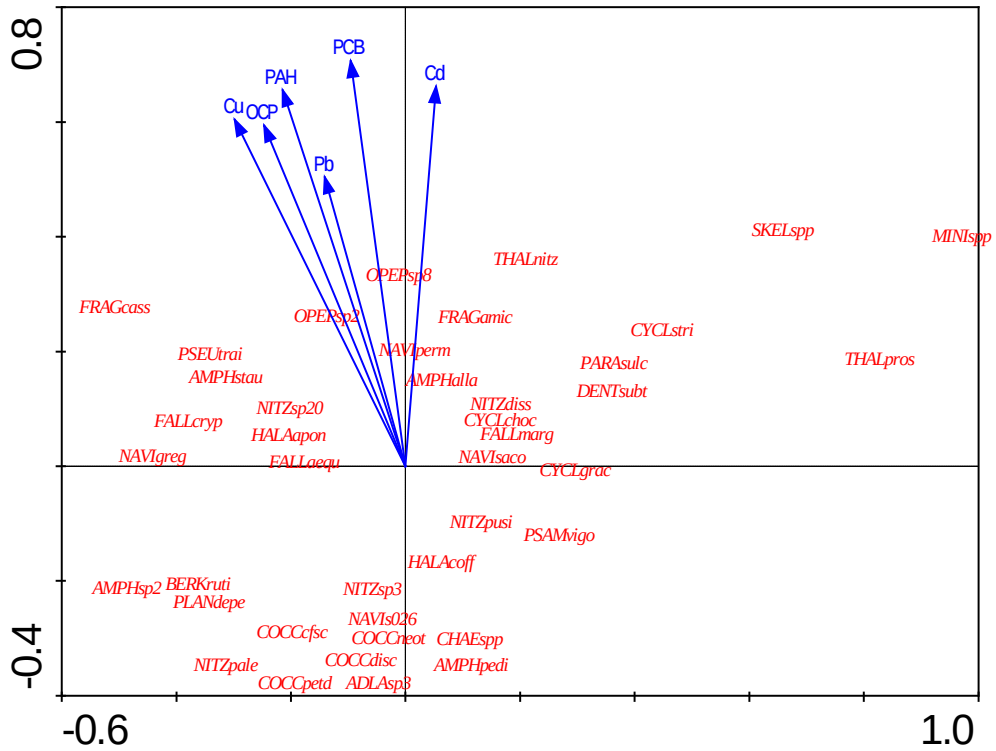

Figure 19. Biplot of species and contaminant variables showing the result of a forward variable selection in CCA, dataset of 50 sites from the Barnegat and Great Bays. Only centroids for species with highest weights (20-100%) are shown. Variables that were

significant at p=0.05 and independently added to the explanatory power of the model were selected and are shown in the plot. Species short codes correspond to those in Appendix 2.

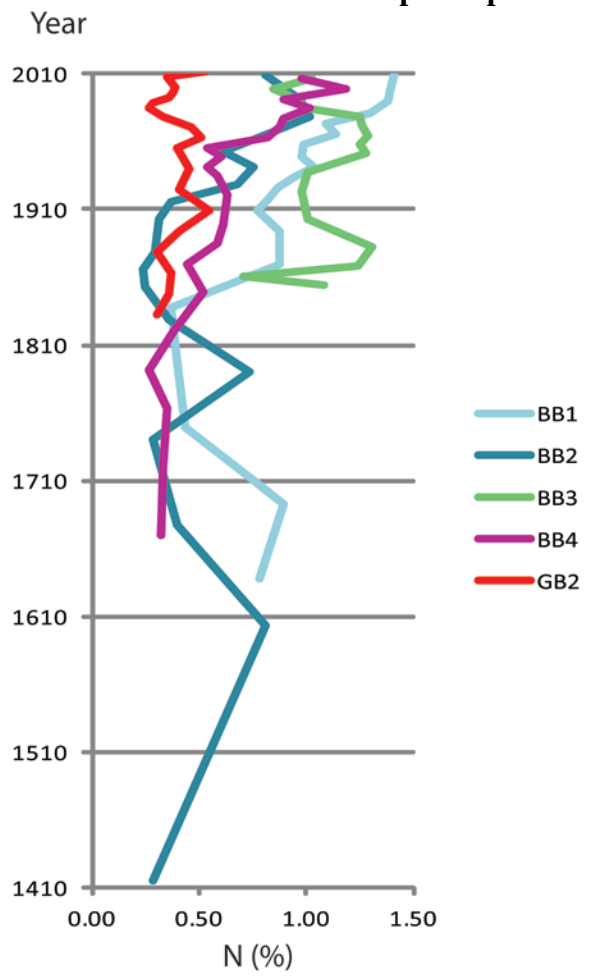

Figure 20. Comparison of temporal changes in Nitrogen content among five sediment cores from Barnegat and Great Bay marshes.

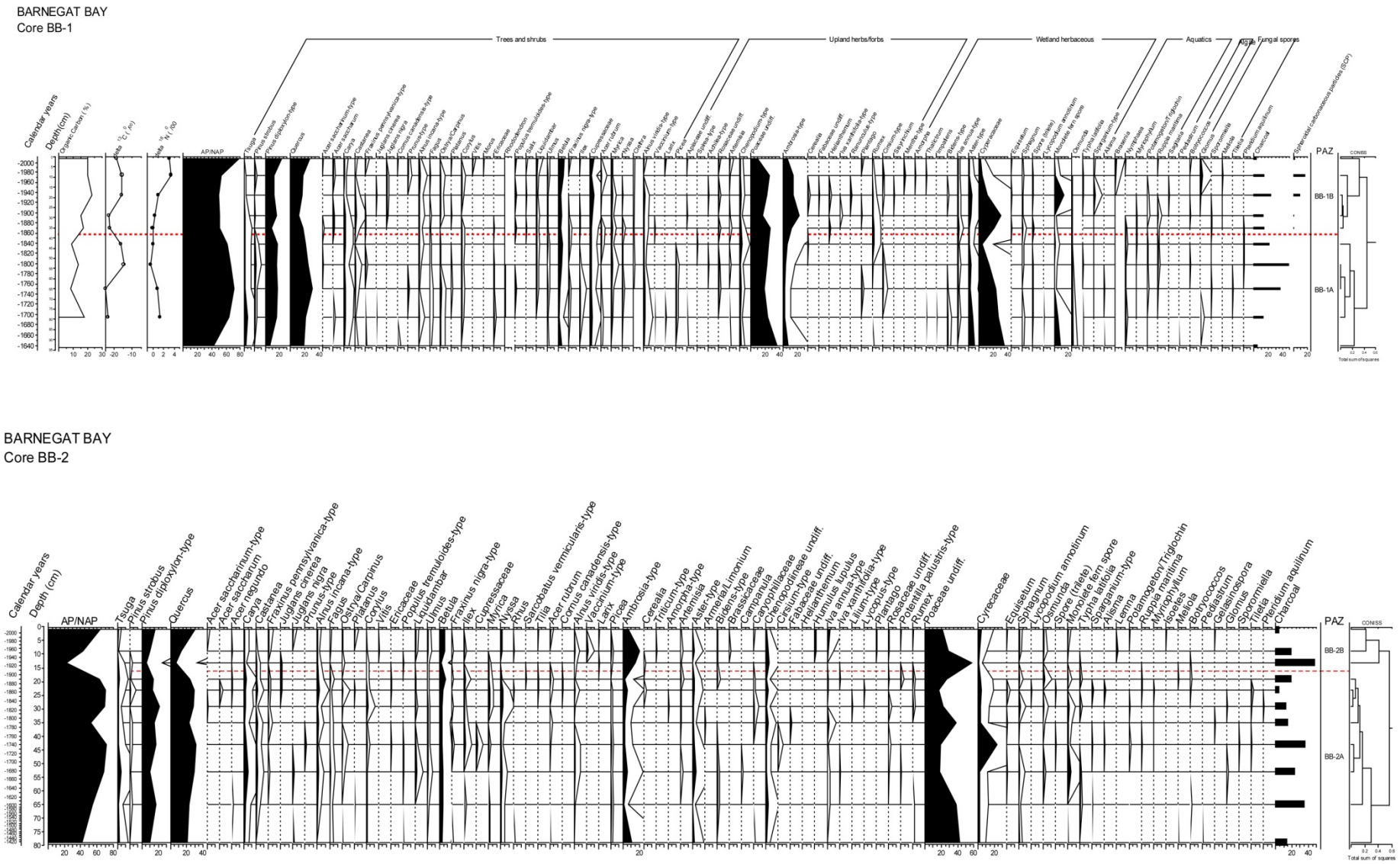

Figure 21. Stratigraphic pollen diagrams for cores BB-1 (upper) and BB-2 (lower).

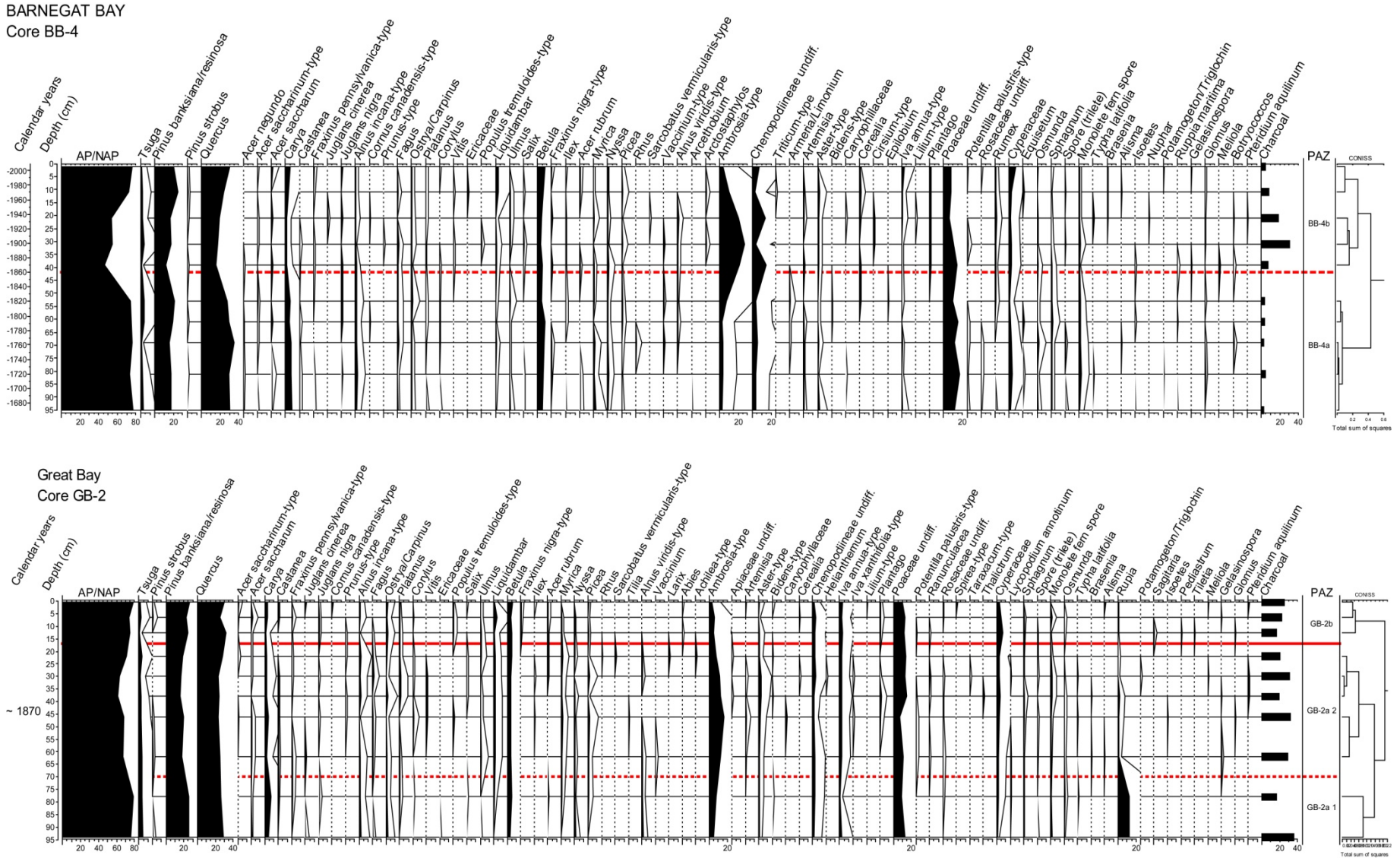

Figure 22. Stratigraphic pollen diagrams for cores BB-4 (upper) and GB-2 (lower).

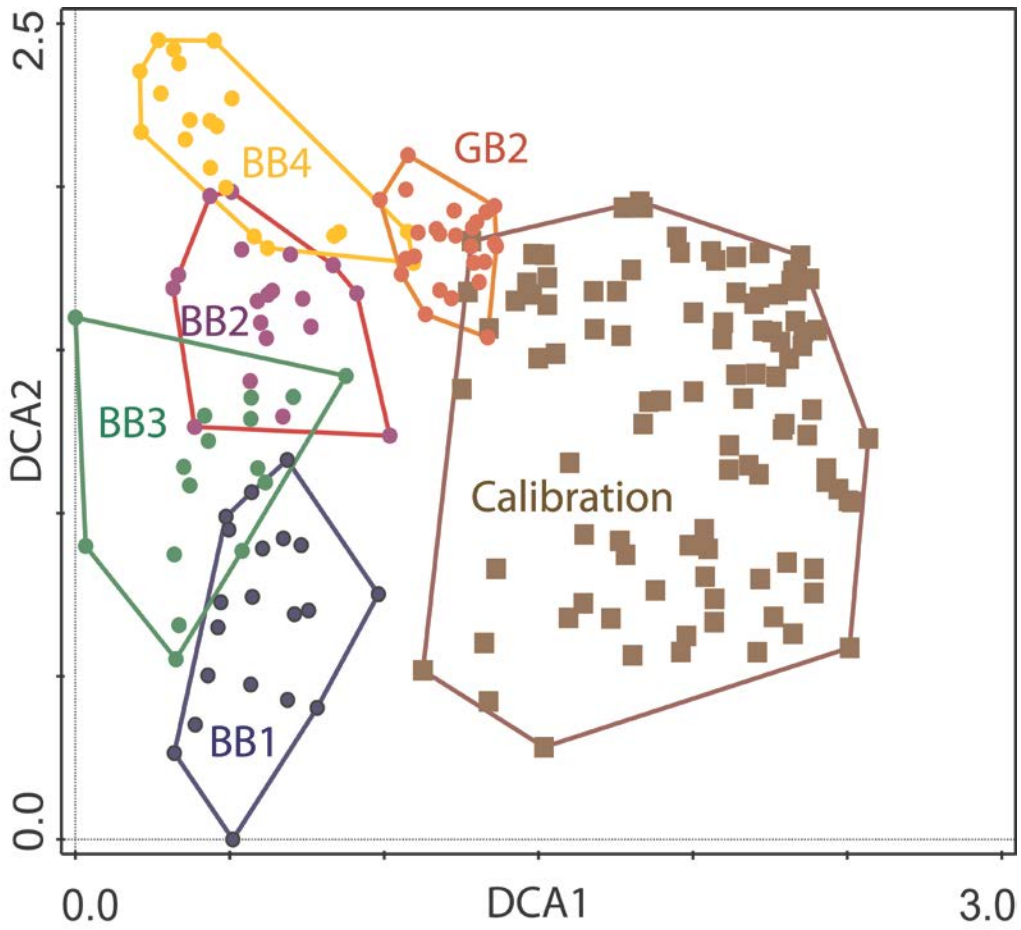

Figure 23. Plot of sample scores in the ordination space of the first and second DCA axes. Samples from the 2012 calibration set are shown by brown squares, core samples – by circles of different colors corresponding to four cores. There is no overlap between samples from the calibration dataset and from Barnegat Bay marsh core samples and only some overlap with Great Bay core. The first ordination axis clearly separated samples from vegetated marshes from those from mudflats, sandflats and subtidal zone, while variation along the second axis was obviously related to salinity, with samples from higher-salinity areas positioned in the upper part of the diagram and those from lower-salinity areas in the bottom part.

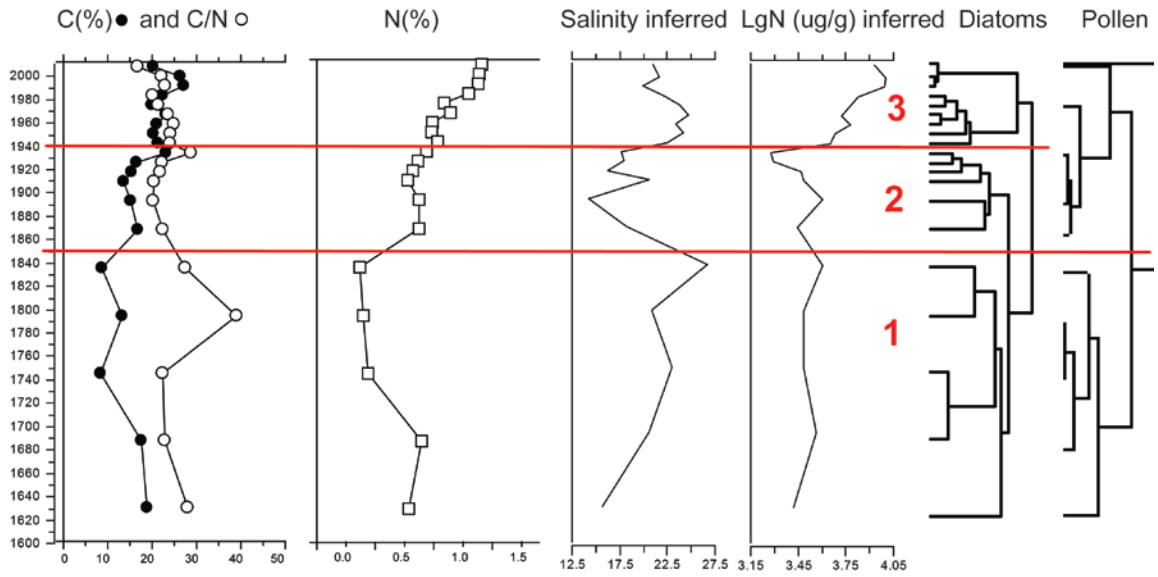

Figure 24. Stratigraphic diagram showing changes along the BB-1 core in sediment organic carbon content (C, %), C/N ratio, nitrogen content (N, %), salinity and nitrogen inferred from diatoms, and major diatom- and pollen base zones resulting from the constrained hierarchical clustering (CONISS). In this core, two pollen zones are evident with the upper zone characterized by an increase in ambrosia pollen. The boundary between these two zones was between 1840 and 1880. The diatom data further divided the upper zone into two with the boundary around 1940. The uppermost diatom zone was characterized by the increased abundance of taxa indicative of high nitrogen content.

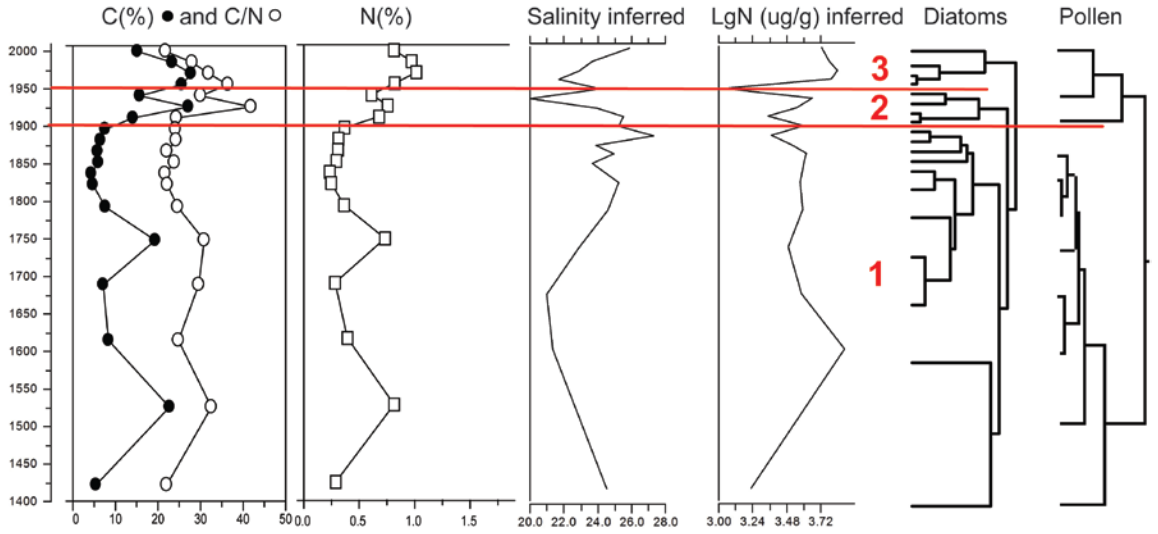

Figure 25. Stratigraphic diagram showing changes along the BB-2 core in sediment organic carbon content (C, %), C/N ratio, nitrogen content (N, %), salinity and nitrogen inferred from diatoms, and major diatom- and pollen base zones resulting from the constrained hierarchical clustering (CONISS). In this core, two pollen zones are evident with the upper zone characterized by an increase in ambrosia pollen. The boundary between these two zones was between 1860 and 1900. The diatom data further divided the upper zone into two with the boundary around 1950. The uppermost diatom zone was characterized by the increased abundance of taxa indicative of high nitrogen content, although the overall trend in inferred N was less evident than in core BB-1.

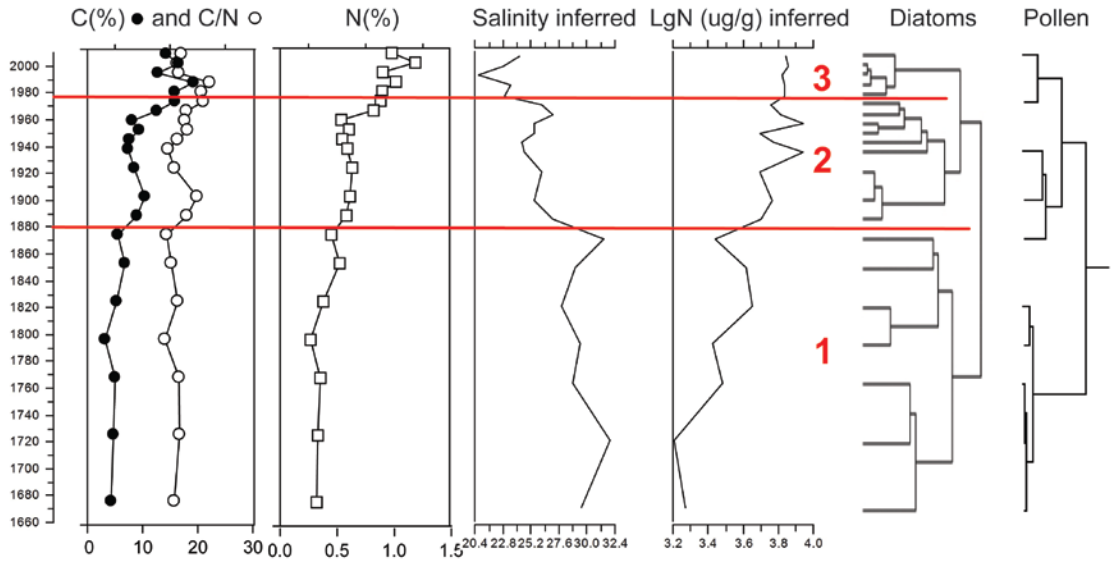

Figure 26. Stratigraphic diagram showing changes along the BB-4 core in sediment organic carbon content (C, %), C/N ratio, nitrogen content (N, %), salinity and nitrogen inferred from diatoms, and major diatom- and pollen base zones resulting from the constrained hierarchical clustering (CONISS). As in the BB-1 and BB-2 cores, the Ambrosia pollen was increased in the upper pollen zone, starting approximately 1860. Three zones could be distinguished from diatom data, but there was an almost continuous trend towards an increase on N-tolerant taxa with time.

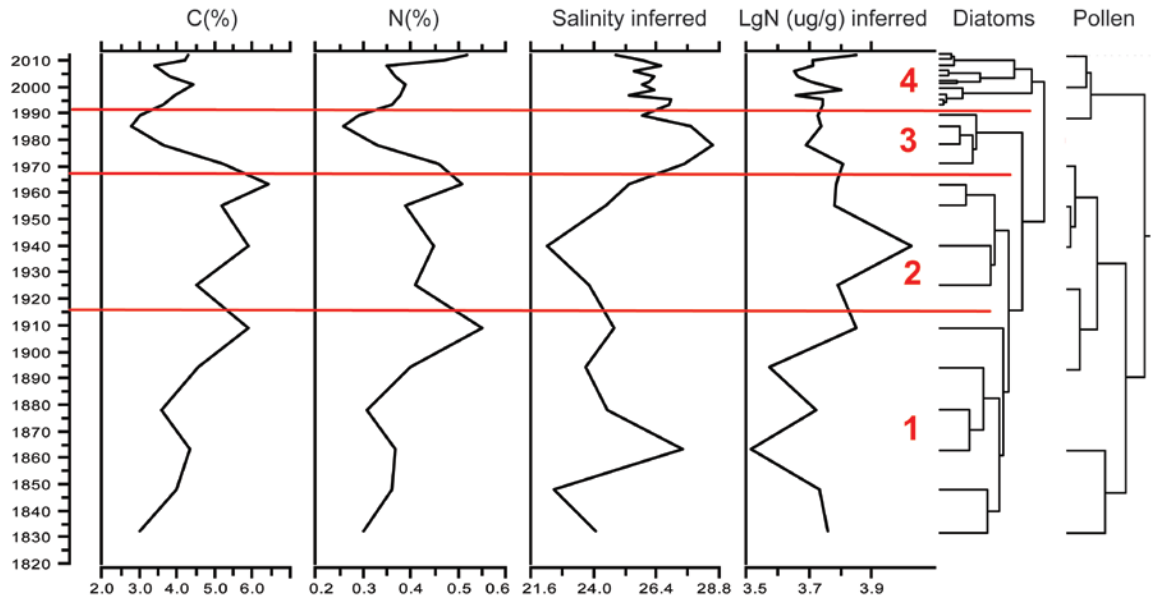

Figure 27. Stratigraphic diagram showing changes along the Great Bay core in sediment organic carbon content (C, %), nitrogen content (N, %), salinity and nitrogen inferred from diatoms, and major diatom- and pollen base zones resulting from the constrained hierarchical clustering (CONISS). Nitrogen content inferred from diatoms was generally following the trend of actual sediment N content, which was in turn practically indistinguishable from C trend.

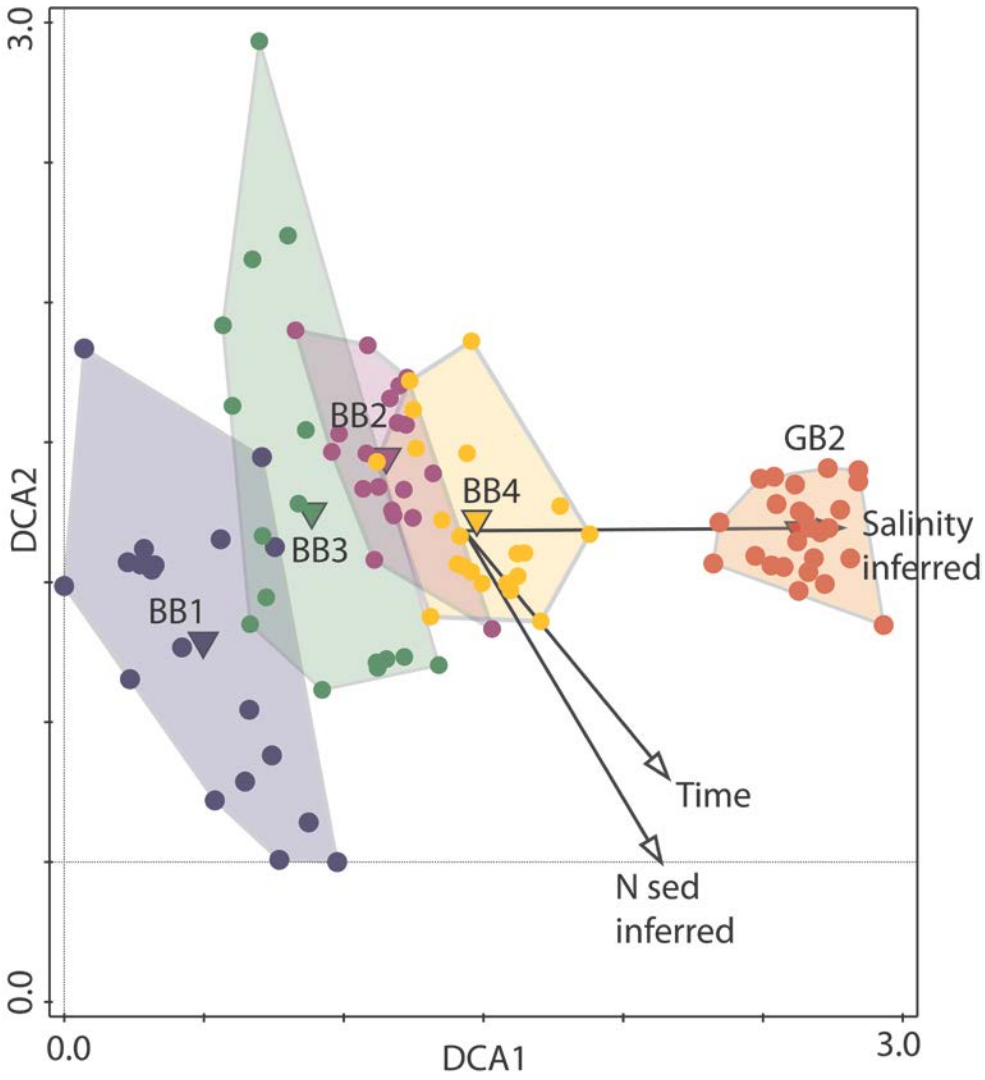

Figure 28. Ordination plot showing sample and core centroids and envelopes around samples belonging to specific cores resulting from a DCA of a dataset of 101 samples from five sediment cores. The arrows show correlations between sample scores and their age, inferred Salinity, and sediment Nitrogen. The diagram shows that although salinity is important in structuring diatom assemblages, the main temporal trend in their species compoisiton is related to the increased nitrogen content in sediments.

Figure 29. Ordination plots showing species centroids, arrows indicating correlations of ordination axes with passive variables (upper plot) and time contour isolines of time (lower plot) resulting from a DCA of a dataset of 101 samples from five sediment cores. Only

centroids for species with highest weights (20-100%) are shown. Time was fitted using the linear LOESS function with span = 0.8 and the robust fitting algorithm in CANOCO 5.0.

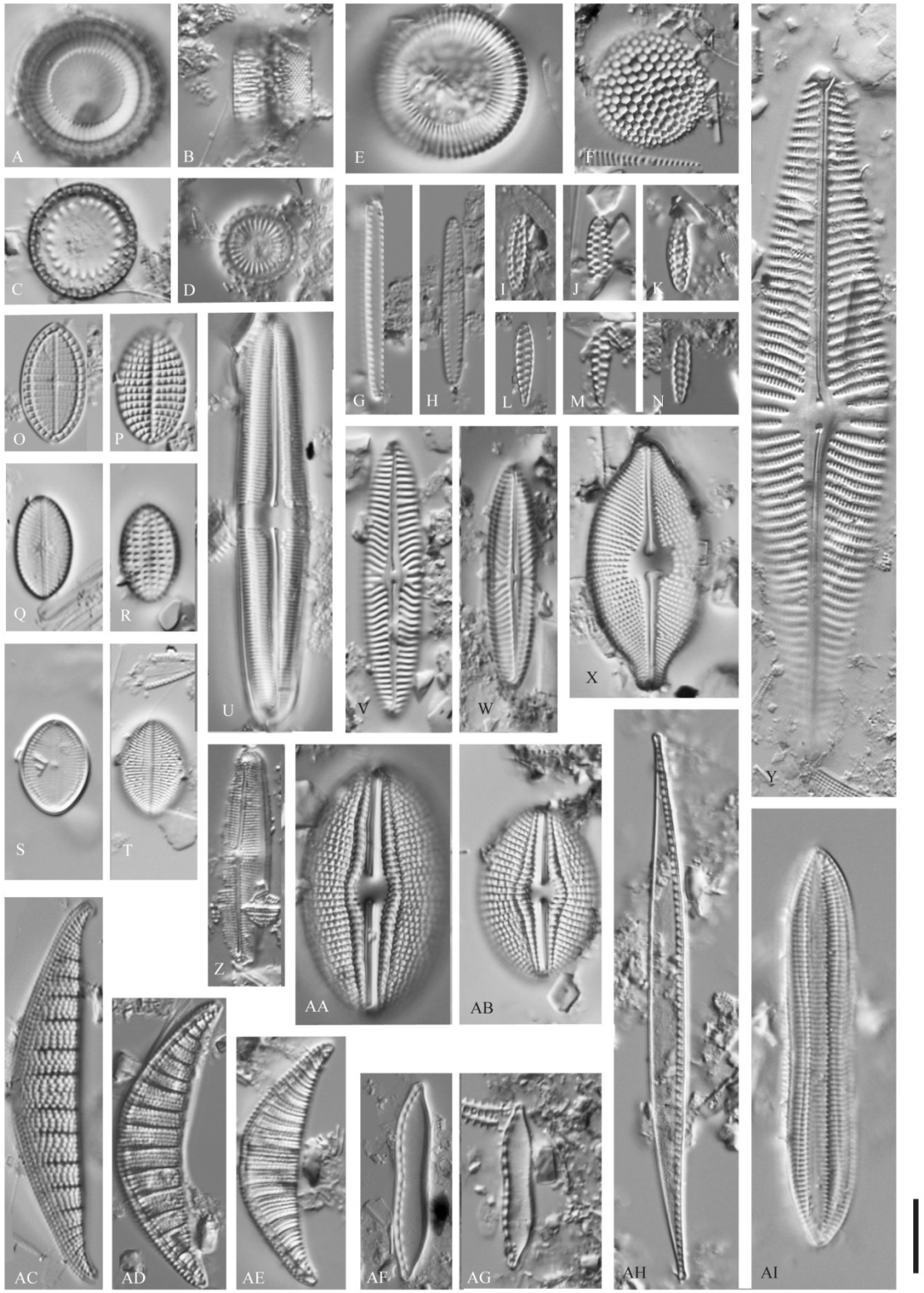

Figure 30. Diatoms characteristic for reference conditions, scale bar=10 µm. A-D. *Paralia sulcata*. E. *Cyclotella striata.* F. *Thalassiosira oestrupii*. G-H. *Thalassionema nitzschioides* Figs I-K. *Cymatosira belgica.* Figs L-N. *Opephora* sp. 2 COAST. Figs O-P. *Cocconeis stauroneiformi.* Figs Q-

R. *C. disculoides* Figs S-T. *C. placentula* var. *lineata* Fig. U. *Caloneis bacillum.* Figs V-W. *Navicula digitoconvergens.* Fig. X. *Cosmioneis pusilla.* Fig. Y. *Navicula peregrina.* Fig. Z. *Frustulia creuzburgensis* Figs AA-AB. *Diploneis smithii* Figs AC-AE. *Rhopalodia acuminata* Figs AF-AG. *Nitzschia brevissima* Fig. AH. *N. sigma* Fig. AI. *N. constricta.*

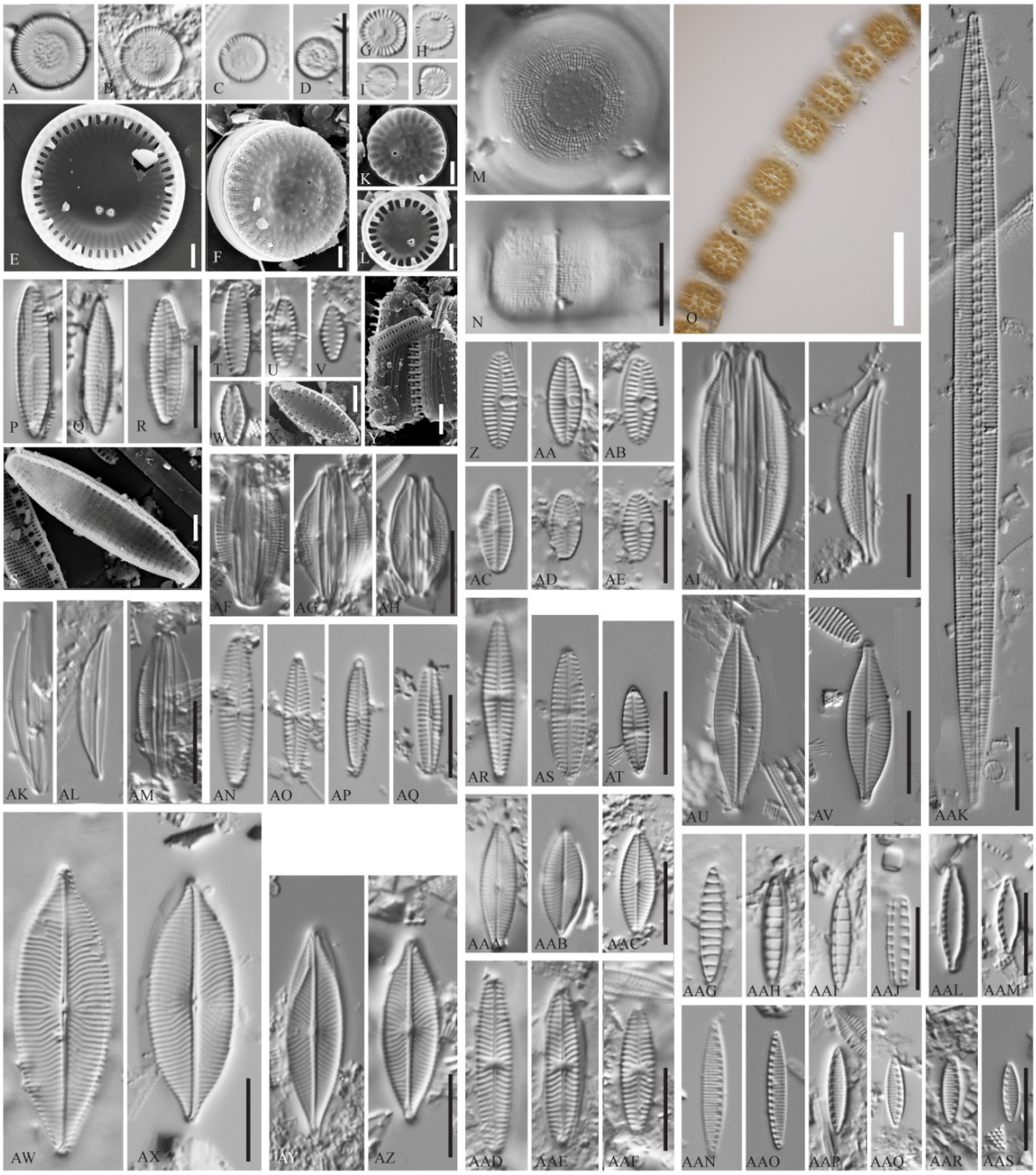

Figure 31. Diatoms that increased in abundance with eutrophication in Barnegat and Great Bay marshes. A-D, G-J, M-N, P-R, T-W, Z-AAS, scale bar=10 µm; LM. Fig. O, scale bar=50 µm; SEM Figs E-F, K-L, scale bar=1 µm; SEM Figs S, X, Y, scale bar=2 µm. A-F. *Cyclotella choctawacheeana.* G-L. *Cyclotella atomus var. gracilis.* M-O. *Melosira nummuloides.* P-S. *Pseudostaurosira subsalina.* T-Y. *Pseudostaurosira* sp. 1 COAST. Z-AE. *Planothidium frequentissimum* AF-AH. *Amphora* sp. 6 COAST. AI-AJ. *Halamphora acutiuscula*. AK-AM. *Halamphora aponina.* AN-AQ. *Navicula salinicola.* AR-AT. *Navicula*

perminuta. **AU-AV.** ***N. gregaria.*** **AW-AX.** ***N. salinarum.*** **AY-AZ.** ***N. jonssonii.*** **BA-BC.** ***N. phylleptosoma.*** **BD-BF.** ***N. microcari.*** **BG-BJ.** ***Denticula subtilis.*** **BK.** ***Bacillaria paradoxa*****. BL-BM.** ***Nitzschia microcephala.*** **BN-BS. N. sp. 20 COAST.**

I) Appendices

APPENDIX 1. Excel file with sediment contaminant data.

APPENDIX 2. Excel file with diatom count data.